BSc Thesis

Study of Freezing and Thawing Processes in Granular Soils

18 June 2024

Author: Yordan Andreev - s2767368

Supervisors: dr. ir.Floriana Anselmucci & Giulia Guida PhD

Second assessor: dr. ir. Bas W. Borsje

UNIVERSITY OF TWENTE.

Preface

The motivation for this research stems from the proposal for a thesis by the Soil MicroMechanics Chair at the University of Twente, aiming to explore the complex behaviour of soil samples subjected to induced freezing and thawing cycles. I would like to extend my gratitude to the Soil MicroMechanics Chair for commissioning this project. Special thanks go to my supervisors for their guidance and support throughout this project, which have been invaluable to the success of this project.

This research has been both a challenging and enlightening journey. This bachelor thesis represents a significant milestone in my academic journey, offering me an opportunity to apply the knowledge I have gained throughout my studies and preparing me for future projects. The process of investigating soil behaviour under freeze-thaw cycles has deepened my appreciation for the complexities of soil mechanics. I hope that the findings of this study will contribute to and inspire further research in this crucial area.

Summary

This study delves into the complex responses of sand-clay mixtures to freeze-thaw (F-T) cycles, a critical aspect of soil mechanics and geotechnical engineering. The research focuses on the volumetric behaviour of these mixtures, with kaolin clay contents varying from 5% to 70%, under controlled F-T conditions. Six samples with 5%, 10%, 20%, 50%, 60% and 70% kaolin were prepared and tested to evaluate the changes in their void ratio, water absorption, frost heave and segregation.

The experimental findings revealed that an increase in kaolin content correlates with higher void ratios and greater water absorption, leading to more significant frost heave. Notably, the finer mixtures exhibited more pronounced volume expansion during freezing, with the frost heave ratio in the second cycle being higher than in the first cycle. Despite some anomalies due to experimental inconsistencies such as sample compaction and water leakage, these observations were mostly consistent with trends identified in a previous study with which a comparative analysis was conducted. Additionally, it was determined that frost heave predominantly occurs in the upper layers of the soil, rather than uniformly throughout the entire sample.

The study concludes that while the experimental results closely approximate real-world soil behaviour under F-T cycles, further research is warranted. Future studies should focus on minimising experimental errors, conducting additional F-T cycles, and improving the simulation of real-world conditions by adopting one-dimensional freezing methods. This research enhances our understanding of soil mechanics, providing valuable insights into the behaviour of granular soils in response to temperature fluctuations.

Table of Contents

1. Introduction

Soil can be characterised as an unconsolidated mixture of mineral grains and decomposed organic material (solid particles), interspersed with liquid and gas occupying the voids between these solid particles. Since the beginning of civilisation soil has been used for various structures. However, it wasn't until the 18th century that the disciplines of soil mechanics and geotechnical engineering were developed (Das & Sobhan, 2014). Since then, these disciplines have been integral to civil engineering.

When talking about soil mechanics one refers to the branch of civil engineering that deals with the study of the physical properties and behaviour of soils, as well as the application of the principles of hydraulics, mechanics and chemistry to engineering problems related to soil. Engineers rely on soil mechanics to predict responses to loads and environmental changes. This makes it essential for designing stable and safe foundations for structures like buildings, bridges, and roads. Understanding soil properties helps engineers overcome issues like settlement, slope instability, and soil liquefaction, hence ensuring the structural integrity and safety of civil engineering projects.

However, the field of soil mechanics encompasses a vast dynamic domain, comprising extensive knowledge that serves as an essential foundation for achieving successful designs. Therefore, it is almost impossible to have a clear understanding of all its aspects. For example, soil is highly complex and distinguishes itself from other construction materials known to humanity by showcasing a broad spectrum of traits, ranging from peats to gravel (Nadeem Akhtar, 2012). Consequently, even within the same location and from identical strata, soil samples extracted from two nearby places can have substantially different properties. Similarly, results obtained from two soil samples taken from the same place but under different weather conditions or applied loads will also exhibit different traits. One such example is soils subjected to freezing and thawing. If engineers want to gain another perspective on soil behaviour it is essential to study how soil reacts to these conditions.

This paper will embark on a comprehensive exploration within the specialised domain of freezing and thawing processes in granular soils. The significance of this research lies in its potential to unravel the hydro-mechanical complexities that emerge within granular soils amidst temperature variations. More specifically this study focuses on revealing the volumetric responses of soil mixtures, specifically those comprised of sand and clay. Insight into these volumetric changes is crucial in engineering as it enhances the understanding of soil properties critical for building stable foundations for structures.

The report is structured as follows. First, the conceptual design is introduced to give more context to the problem at hand. This chapter consists of several sections such as research motivation, involved parties and research objective, all of which aim to provide a clearer picture to the reader of the task to be done. In the next chapter, the dimensions of the research process are presented, including the aims and scope of the project as well as the research questions. These dimensions play a pivotal role in setting up the rest of this project. Based on the dimensions, a research framework is developed in Chapter 4 to outline the steps needed to execute the assignment and guide the research process. Chapter 5 contains the technical design and the methodologies that will be used to answer the research questions and elaborate on the framework from the preceding sections. Following that, Chapter 6 explains how the experimental campaign was conducted and characterises the samples. Chapter 7 looks into the results from the experiments and provides a comparative analysis with previously obtained results from a similar study. Finally, the last

three chapters provide an overview of the findings from this research and give recommendations for improvements in future research in the field.

2. Problem Context

2.1. Problem Statement

The transformation of pore water into ice when temperatures fall below the soil mixture's freezing threshold significantly alters the soil's hydro-mechanical characteristics. This process leads to an expansion within the soil particles due to the lower density of ice, accompanied by the migration of pore water towards the frozen front. The reverse thawing process rarely restores the initial unfrozen state because of the microstructural changes that occur during freezing. Prior research has shown that the volumetric changes are mainly influenced by the fine content and the water availability (Benkelman & Olmsetead, 1932). The reasons for volume expansion in frozen soils go beyond the lower density of ice compared to liquid water - 0.917 g/cm^3 in comparison to 0.999 g/cm^3 (Valves Instruments Plus Ltd, n.d.). Interface tensions at the freezing front are another reason by causing water migration and accumulation, leading to the formation of ice lenses (Penner, 1959). The presence of very fine grains in the soil appears to be a critical factor in reducing pore sizes thus leading to a rise in interface tensions and influencing ice segregation, with minimal segregation occurring in soils with lower concentrations of such fine particles. However, there is limited knowledge about the exact frost heave volume response of soil mixtures, necessitating further insight into the effects of the freezing and thawing processes.

2.2. Research Motivation

Unstable soil or wrong assumptions about soil characteristics can pose serious risks to the structural stability of buildings. Therefore, understanding soil properties is crucial for engineers to make informed decisions during the design and construction phases. This ensures proper foundation support, building integrity, and mitigation of potential issues related to soil movement or instability. Specifically, when freezing temperatures induce the transformation of pore liquid water into ice, a series of hydro-mechanical phenomena ensues, affecting the soil's overall behaviour. The expansion of soil volume caused during freezing, known as "frost heave," and the settlements experienced by ice-rich soils are critical for the stability and performance of structures and infrastructure in cold regions (Hjort et al., 2022). Understanding the repercussions of these freezing and thawing processes in soils is only one aspect of comprehending soils' responses to various conditions. Nonetheless, this knowledge could be of great use to future engineers and researchers as well as to foster advancements in sustainable and resilient infrastructural development, which is the reason for choosing to execute this particular project.

2.3. Involved Parties

The Soil MicroMechanics Chair at the University of Twente, within the Department of Civil Engineering & Management (CEM), commissioned this project. The findings from the project may be valuable to various parties around the world involved in construction and engineering practices in regions prone to frost heave or artificial ground freezing, as well as to the CEM Department at UTwente for education and research purposes. By haining a deeper understanding of the soil's volumetric response under (controlled) freezing and thawing processes, methods for predicting and preventing the instability of earth (infra)structures will become more accurate and reliable. Thus, several stakeholders, including the University of Twente, consultancy and engineering companies, municipalities, and students, may benefit

from this research. Additionally, resident in areas frequently affected by freezing and thawing processes in can also be classified as stakeholders due to their fundamental need for a safe urban environment.

2.4. Research Objective

Given what has been mentioned already, the objective of this research is to expand the understanding of the volumetric behaviour of sand and clay mixtures under freeze-thaw cycles by studying the impact of these cycles on granular soils through an analysis of results from experimental campaign and comparison with previously obtained results of 3D+time images made with X-ray tomography.

3. Research Dimensions

3.1. Research Aims

This research includes several aims all of which are required for the successful completion of the project. They can be summarised as follows:

- The first aim is to focus on selecting the soil compositions consisting of sand and clay that will be tested, and characterising them.
- The next aim consists of designing and conducting an experimental campaign to observe how the chosen porous media behave under continuous cycles of freezing and thawing.
- The third aim is to analyse how the microstructure of soil and ice evolves after being subjected to freezing and thawing cycles.
- The last goal is to compare the findings to results acquired in a previous study with the same objectives and to gain a further understanding of the behaviour of soils.

3.2. Research Scope

The soil compositions vary in sand-to-clay ratios and void ratios. The experimental campaign involves determining optimal sample features, test duration, temperature conditions, and monitoring methods. Laboratory experiments are performed to regulate external factors and all variables, ensuring the reproducibility of the research and bolstering its credibility. The examination of the results is directed to the alterations in the behaviour of granular soils. An analysis that encompasses the response of various soil mixtures to freezing and thawing is conducted. Finally, an image-processing approach using the Fiji processing tool is applied to compare the results to 4D images (3D + time) containing different results.

3.3. Research Questions

Several research questions follow from the research objective and framework. This research is going to answer the following questions:

1. What different mixtures of sand and clay can be used and how do their characteristics differ?
- Prior to conducting any experiments, it is essential to identify the specific soil mixtures that will be tested based on varying sand-to-clay ratios. This requires the formulation of a methodology that can be used to characterise their main physical features. Following that they need to be characterised.

2. What is the best way to conduct experiments involving cycles of freezing and thawing in order to determine the volumetric response of granular soils?
- Four subquestions can be formulated here:
  - ❖ How many tests should be conducted?
  - ❖ What should be the temperature for the freeze and thaw cycles?
  - ❖ What should be the test durations of the experiments?
  - ❖ How will the experiment be monitored and measurements taken?

3. How do the results from the experiments compare to previously obtained data from 4D image reconstructions using X-ray tomography?

- The results can be analysed by answering the following subquestions:
    - ❖ How does void ratio change throughout the experiments?
    - ❖ What is the observed frost heave of the soil after the application of the freeze-thaw cycles?
    - ❖ How much water absorption is there during freezing?
    - ❖ Does any segregation in the soil appear?
    - ❖ Are there collapses during thawing?
    - ❖ Are there similarities to other independent results?

4. Research Framework

A methodology of the research framework needs to be formulated to provide a general idea of what steps need to be taken. To demarcate all phases of the project, the research framework will present all objects required to achieve the objective of the research. Moreover, it will be explained how these various objects are related to each other. The framework is organised as a scheme and can be seen in Figure 4.1 below.

Outcome/Objective: The outcome as shown in the rightmost red box in the figure is to expand the knowledge of soil volumetric changes after freezing and thawing (F-T) cycles.

Research Objects: Several objects (boxes in blue in the figure) are present. The two main objects directly leading to the outcome are the insight into how soils behave during freezing and thawing. Preceding them, are the rest of the objects that are necessary. All of them should be acquired before the experiments can be conducted. The first one - "Mixture characteristics" - is related to the soil samples that will be tested and is the foundation of the experiments as different soil characteristics can lead to drastic changes in the results. The other four objects determine how the experimental procedure will go, how many cycles will be tested, how long it will take and how it will be examined.

Criteria: The criteria (boxes in purple) are used to depict how the objects will be assessed and to link them to each other. The different soil mixtures are distinguished based on their void and sand-to-clay ratios, as well as repose angles. The experimental campaign will be assessed by determining the ideal number of freeze and thaw cycles based on the time available, the minimum (T min) and maximum (T max) time for these cycles, choosing a reliable monitoring method, and appropriate temperatures for the cycles. Once the results are reached, the samples will be assessed based on six criteria: water absorption, frost heave, void ratio changes, segregation, sample height changes and any potential collapses. Following that, the results will be analysed and compared.

Sources: The left side of the diagram (boxes in green) illustrates the main sources that will be used to gain information while working on the project. These will mainly be various scientific papers and results from the experiments, however, the received feedback on the project will also be vital.
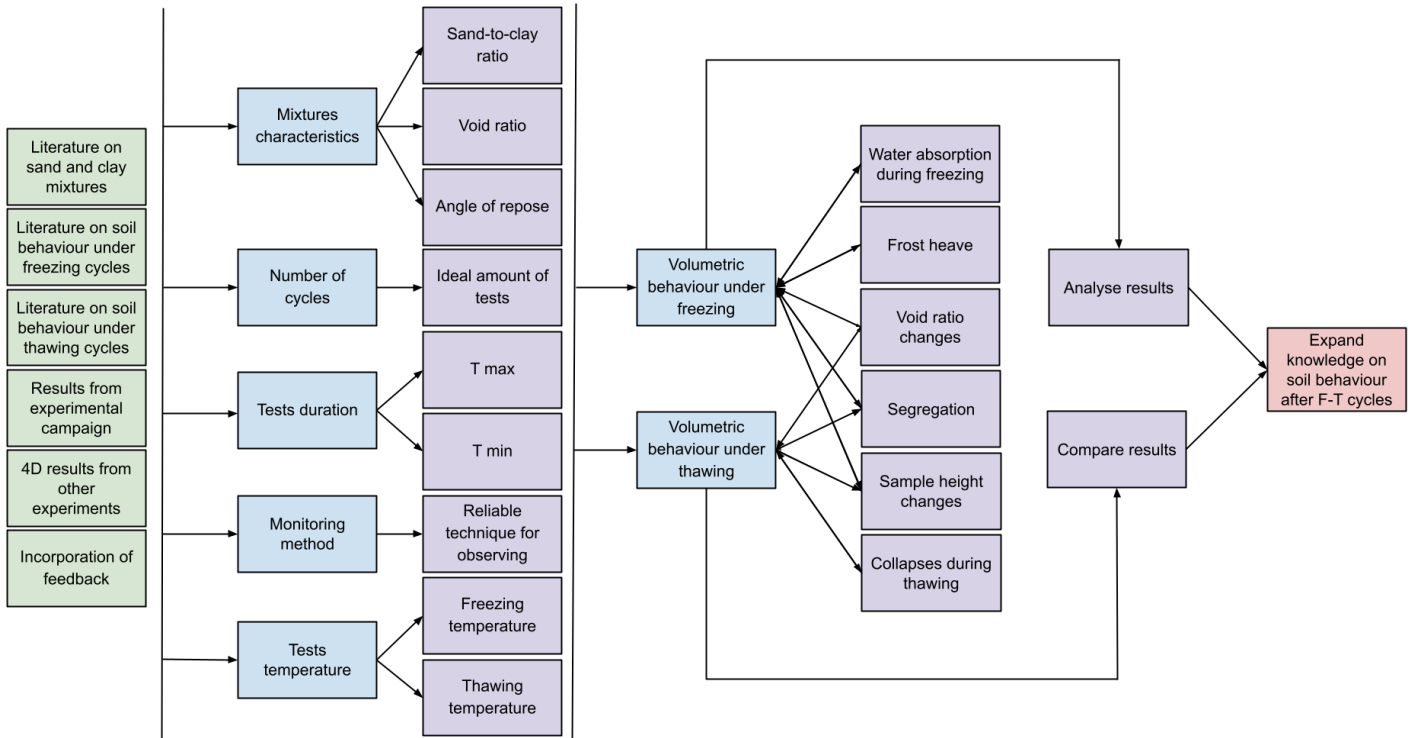
Literature on sand and clay mixtures

Literature on soil behaviour under freezing cycles

Literature on soil behaviour under thawing cycles

Results from experimental campaign

4D results from other experiments

Incorporation of feedback

Mixtures characteristics

Number of cycles

Tests duration

Monitoring method

Tests temperature

Sand-to-clay ratio

Void ratio

Angle of repose

Ideal amount of tests

T max

T min

Reliable technique for observing

Freezing temperature

Thawing temperature

Volumetric behaviour under freezing

Volumetric behaviour under thawing

Water absorption during freezing

Frost heave

Void ratio changes

Segregation

Sample height changes

Collapses during thawing

Analyse results

Compare results

Expand knowledge on soil behaviour after F-T cycles

Figure 4.1: Research framework (green - sources of information; blue - research objects; purple - criteria; red - research objective)

5. Research Methods

This chapter elaborated on the research methods applied and their role in obtaining the desired answers. By setting the stage for addressing the research questions, the methods encompass all main aspects of the project, including a suite of experimental and analytical techniques adopted in the research. These methods involve performing laboratory tests, encompassing sample preparation and freezing and thawing cycle measurement. An analysis to interpret the experimental results is also conducted. Image processing procedures utilised for comparison to independent results is the final aspect of the research methods.

1. What different mixtures of sand and clay can be used and how do their characteristics differ?

Often in the past, both experimental and theoretical studies of soil behaviour have focused on ideal soils, i.e. pure clay and uniform sand. Consequently, soil mechanics has largely evolved from analysing test results obtained from these ideal soils (Yin et al., 2021). However, natural soils are much more complex and can not always be accurately replicated in experiments. Therefore, to better understand the characteristics of these natural soils, more simplified soil mixtures are typically used in laboratory testing. Usually, the simplified soils are made of coarse-fine mixtures. Often these include sand and clay, which are also the materials used in this research.

The specific type of clay used to form the mixtures is kaolin Speswhite clay. It was chosen because kaolin is one of the most abundant clay types found in nature and is widely distributed (Čejka et al., 2017). The second component of the mixtures is fine sand. Furthermore, much research and literature is available on sand-kaolin mixtures, providing the groundwork for additional studies and comparisons. Since the amount of fines in the mixture heavily influences soil characteristics and greater fines content heightens frost susceptibility (Konrad & Lemieux, 2005), several soil samples with altered sand-to-clay ratio is examined to confirm this relationship and understand its specific implications.

Four of the mixtures that are tested contain the same amounts of coarse and fine particles as the mixtures used in the comparison experiment. This is done in order to conduct a more accurate and meaningful comparison with the results in the end. These soil mixtures consist of 50%, 80%, 90% and 95% sand content. Additionally, to test the effect that higher clay contents have on frost heave, two more mixtures for which the sand comprise 40% and 30% of the mixture, respectively, are tested, resulting in 6 different soil mixtures. When a mixture is described as having 95% clay content, it means that 95% of the total weight of the mixture is clay. The soil mixtures are kept in transparent perspex cylinders with an inner diameter of 3 cm. However, the process of soil preparation and human error can sometimes lead to inaccuracies in measurement or inconsistent testing results. Therefore, the methodology for this research is to replicate the tests for each of the 6 samples two times under the same conditions to study their repeatability. This way the results of the changes in soil properties from the first trials can be verified.

In addition, the water content of the soil mixtures plays an important role in the outcome of the experiments. To replicate real-world scenarios where soils are completely saturated with water, which is usually the case in colder regions due to melting snow or precipitation, all soil mixtures are tested in fully saturated conditions, i.e. 100% water content in the pore spaces. Saturated soils are more vulnerable to frost action compared to partially saturated or unsaturated soils, making the data gathered from experiments with this level of water saturation more insightful about the the reaction of the soils.

Moreover, using the same water content for each mixture makes them more easily comparable. To achieve full saturation, all mixtures are submerged in containers filled with water, thus allowing water to seep into the soil through the bottom permeable end of their cylinders. The samples are left submerged for 20 hours to guarantee complete saturation and that they are under vacuum. Additionally, a film of 1 cm of water is left on top of each sample because water availability is essential for frost heave to develop.

Determining the angle of repose of the mixtures is also important for characterising them. The angle of repose refers to the angle of the steepest slope of a stable mount of granular material formed under gravity without collapsing. In other words, it is defined as the angle between the cone slope and the horizontal plane when bulk cargo is poured onto this plane. This angle varies depending on factors such as the size, shape, and cohesion of the particles (Beakawi Al-Hashemi & Baghabra Al-Amoudi, 2018). To estimate the angle of repose the fixed funnel method shown in Figure 5.1 can be utilised. In this method, the materials are poured from a funnel at a certain height. The funnel is then raised slowly while the conical shape of the pile is forming to keep the dropping height constant and minimise the effect of the falling particles. When the pouring of the material is stopped the angle of repose is measured with Equation 1.

$$\theta = atan(2H/D) \hspace{4cm} Equation\ 1$$

Where:
- θ - angle of repose [°]
- H - maximum height of the piled material [cm]
- D - average diameter of the formed conical shape [cm]
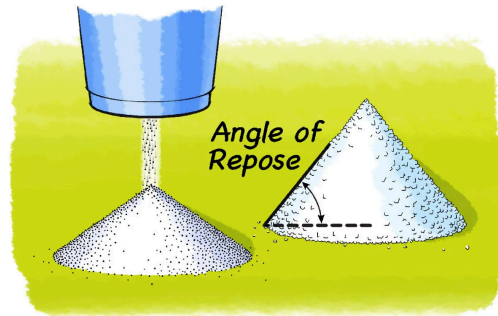
Figure 5.1: Angle of repose (Lohner, 2019)

Furthermore, with the changes in fine content, the void ratio also change for each mixture. Studies by Phan et al. (2016) and Lade et al. (2009) indicate that the void ratio may slightly decrease initially for very small percentages of fine particles, but it gradually rises as the fine content increases. During freezing, higher amounts of water in the soil due to greater void content can lead to a more significant expansion of ice within the soil and enhance frost heave. Therefore, it is essential to characterise the mixtures based on void ratio and to consider its influence on the soils' reaction to freeze-thaw cycles. Hence, the voids are examined at the beginning and the end of the experiments, as well as for each stage of the experimental campaign, i.e. after every freezing and thawing process. The void ratios can be calculated using Equation 2:

$$e = \frac{V_V}{V_S} \hspace{4cm} Equation\ 2$$

Where:

- e - void ratio [-]
- V_V - volume of voids [cm³]
- V_s - volume of solids [cm³]

The volumes used in the equation are determined by first measuring the dry masses of the sand and kaolin in the mixtures before mixing. The mass is then used to calculate the volumes. The volumes of the solids (i.e. volume of clay solids and volume of sand solids) are found by inverting and applying Equation 3 to the two components of the mixture separately. In the equation, the density of the solids is found through a literature review.

$$\rho_s = \frac{M_{d\_S}}{V_S} \qquad \qquad Equation\ 3$$

Where:
- M_{d_s} - dry mass of solids [g]
- ρ_s - density of solids [g/cm³]
- V_s - volume of solids [cm³]

Having found the volume of the solids, it can be subtracted from the total volume of the soil sample to determine the volume of voids:

$$V = V_V + V_S \Rightarrow V_V = V - (V_{clay} + V_{sand}) \qquad \qquad Equation\ 4$$

Where:
- V - total volume of sample [cm³]
- V_V - volume of voids [cm³]
- V_s - total volume of solids [cm³]
- V_{clay} - volume of clay solids [cm³]
- V_{sand} - volume of sand solids [cm³]

Consequently, we can go back to Equation 2 and determine the void ratios. To visualise the differences between the different mixtures, a "Void ratio vs Fines percentage" graph can be created. To characterise the mixtures, the minimum and maximum void ratios of each mixture are determined. The maximum void ratio can be calculated when the soil is in a loose state. In this state, the soil occupies its maximum total volume, resulting in the highest void ratio. Conversely, the soil can be compacted to decrease its volume and obtain the minimum void ratio. By applying the aforementioned equations to both scenarios, the two extreme void ratios can be estimated.

2. What is the best way to conduct experiments involving cycles of freezing and thawing in order to determine the volumetric response of granular soils?

It is imperative to thoroughly examine and discuss each of the four subquestions.

❖ How many tests should be conducted?

By reviewing existing literature on similar experiments and studies, insight into typical ranges of freeze-thaw cycles used in similar materials and conditions can be found. This can serve as guidance for determining how many cycles to apply in this research. Various studies use a different number of

freeze-thaw cycles ranging from 3 in Konrad and Lemieux (2005) or 7 in Huang et al. (2022) up to 12 cycles in the "Influence of freeze-thaw cycles on mechanical properties of a silty sand" study by Liu et al. (2016). Conducting a larger number of cycles may provide more comprehensive data on the susceptibility of the material to frost heave. However, accounting for the time constraints of the assignment, which spaned 10 weeks with only 3 or 4 weeks allocated for conducting experiments since the rest are needed for analysing the results, testing for 2 cycles appeared to be the most optimal and feasible choice.

❖ What should be the temperature for the freeze and thaw cycles?

The freezing process consists of placing the cylinders with soil mixtures in a freezer where the temperature is be maintained at approximately -5°C throughout. Additionally, to simulate freezing conditions closer to reality, the perspex cylinders are wrapped laterally with an insulation coating to prevent or at least minimise lateral thermal dispersion and ensure that heat transfer will primarily occur in one dimension (from top to bottom) within the soil mixture during freezing. For the insulation, the material used is Armaflex insulation for pipes (see Figure 5.2). During thawing, the mixtures are taken out of the freezer and allowed to defrost at room temperature. For these processes, the top of the cylinders are left open in contact with the environmental temperature.

Figure 5.2: Armaflex insulation for pipes (EnergyMall, 2021)

❖ What should be the test durations of the experiments?

Given that the soil samples are stored in small containers, it is reasonable to assume that they will freeze relatively quickly. However, complete freezing of the samples is crucial. Thus, the testing program is designed to include a freezing process lasting 18 hours. The defrosting of the soil is expected to require less time. Assuming that 4 hours are sufficient for the thawing process, this will make for an overall 22-hour test cycle. It is crucial to maintain a consistent cycle duration in order to achieve more accurate results and to ensure that any variations in the outcomes are due to the desired changes in experimental conditions, rather than differences in timing. This consistency reduces potential sources of error and enhances the reliability and comparability of the results. Considering that the cycles take a long time, 6 soil samples are tested simultaneously.

❖ How will the experiment be monitored and measurements taken?

During and after each stage of the experiment pictures of the soil samples are takenboth after soil preparation and following each thaw or freeze process. These images are used to conduct a visual analysis of the soils and detect any noticeable changes such as soil segregation, collapses and formation of ice lenses. In addition, the deformations in the soil such as heave height or alterations in the thickness of the water film are measured with a calliper and tape measure.

3. How do the results from the experiments compare to previously obtained data from 4D image reconstructions using X-ray tomography?

The analysis of the experiments includes answering each of the subquestions separately.

❖ How does void ratio change throughout the experiments?

As explained before, it is important to understand how the void ratio evolves with each stage of the experiments due to its impact on the frost heave. After every freeze-thaw cycle, the total volume of the samples changes leading to different volumes of voids and subsequent different void ratios. By measuring the total sample volume after each step and utilising Equations 2 to 4, the changes in void ratio can be calculated. Thus evolution can be shown by developing "Void ratio vs Time" graphs for all mixtures.

❖ What is the observed frost heave of the soil after the application of the freeze-thaw cycles?

The methodology for determining the heave of the samples is centred on the frost heave ratio. It is defined as "the proportion of frost heave increment over the depth of the whole sample" according to She et al. (2018). This ratio is a useful metric for evaluating the frost heave susceptibility of the soil samples. It provides a numerical value that allows for an easy comparison between different samples or experimental conditions. Moreover, the frost heave ratio normalises the measurement by expressing the volume increment as a percentage of the initial height of the soil sample. As a result, it becomes independent of sample size or heights, enabling direct comparison between samples of varying depths. The ratio is given by Equation 5:

$$\eta = \frac{\Delta h}{h_0} * 100\% \hspace{4cm} \textit{Equation 5}$$

Where:
- η - frost heave ratio [%]
- Δh - increment/height of the frost heave [cm]
- h_0 - depth of the sample [cm]

The increment of the frost heave in the equation refers to the elevation increase of the soil surface caused by frost heave. This height difference between the initial and elevated states of the soil surface is measured after each freezing and thawing phase. Since the sample height directly influences frost heave, it is important to monitor how it changes throughout the experiment.

The results from the frost heave analysis are plotted and shown in the form of several graphs, yielding a crucial way for comparing the outcomes. The graphs include:
- Heave ratio (%) vs Fines (%)
- Heave ratio (%) vs Number of F-T cycles (-)
- Heave ratio (%) vs Void ratio (-)

❖ How much water absorption is there during freezing?

To estimate the absorption during freezing, first, the thickness of the film of water at the top of the sample before and after each freezing test are measured. The decrease in the water film thickness corresponds to the amount of water absorbed. However, for better data interpretation, the water absorption is quantified

based on the volume of water absorbed. The change in the thickness are used to calculate the amount of water absorbed. This is calculated with Equation 6:

$$\Delta V_{abs} = A * \Delta h \qquad\qquad Equation\ 6$$

Where:
- A - cross-sectional area of the cylinder [cm^2]
- Δh - change in thickness of the water film [cm]
- ΔV_{abs} - volume of water absorbed [cm^3]

❖ Does any segregation in the soil appear?

Soil segregation occurs when soil particles separate or sort based on their size, shape, density, or other properties, leading to the formation of distinct layers within the soil. Segregation often coincides with the development of ice lenses. Ice lenses are thin, lens-shaped layers of ice that form within the soil (see Figure 5.3). In the figure below, the frozen fringe is the zone at which the ice lenses begin to form. During the freezing of fine-grained soils, suction arises at the frost line (Saetersdal, 1981). This process causes water to migrate through the soil pores and accumulate at the freezing front, where it freezes and forms ice lenses. As the water migrates and freezes, it can transport and segregate soil particles.
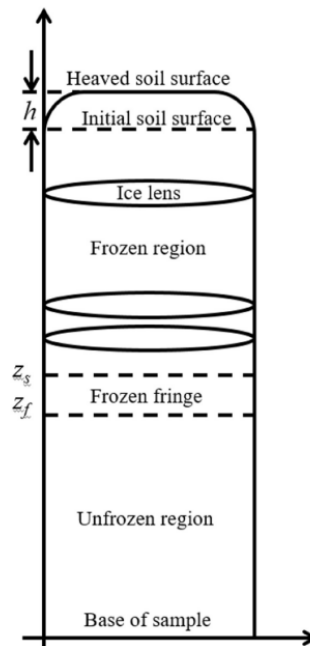
Figure 5.3: Changes in soil during freezing (She et al., 2018)

The samples undergo visual inspections to detect segregation. By taking pictures before and after each thawing-freezing cycle and examining them for signs of separation in the soil, segregation can be determined to have transpired. Besides the formation of ice lenses, other indicators for segregation can be distinctive patterns of surface cracking or deformation or layering of different soil components. For instance, freezing and thawing processes can create aggregate bands, where particles with similar size, shape, porosity, or density cluster together.

❖ Are there collapses during thawing?

Sudden collapses in soil often result from segregation processes. When soil freezes and ice lenses form, the presence of ice enhances cohesion and stability by binding soil particles together. However, the ice fronts also separate the soil in sections. During thawing when the ice melts, it leaves behind large void spaces or cavities that become saturated with water. Over multiple freezing and thawing cycles, these void spaces can weaken the soil structure (Guoyu et al., 2011), compromising its structural integrity and making it susceptible to collapses or settlements.

Collapses during the thawing of the soil mixtures can be detected through simple observation for signs of major soil movements or shifting. Localised sinkholes are one indicator of the occurrence of collapses. Other signs of collapses can be concave or crater-like features on the soil surface. Additionally, since the tests of each soil sample are replicated 3 times, consistency in soil settlement across these replications is expected. By comparing the post-thaw appearance of the soil in each replication, any notable deviations between the three test runs may signal potential collapses in the test that differs from the other two. It is expected that collapses should be mostly observed for the mixtures with higher fine content.

❖ Are there similarities to other independent results?

Finally, the experimental findings are compared with results obtained from previous research conducted using a similar methodology to the one applied here. Therefore, this comparative analysis aims to validate the accuracy and reliability of the produced results in this thesis. Consistency between the two sets of results should enhance the confidence in the findings and strengthen the robustness of the conclusions drawn from the experiments.

The independent results for the comparison are provided by the supervisors of the project from the Soil MicroMechanics Chair. They are in the form of three-dimensional images taken with X-ray tomography tools and represent the different deforming stages of the soil mixtures under freezing and thawing. These results undergo image processing, for which the Fiji processing software is used and python codes are developed. After the images are processed and interpreted, they are compared to the diagrams that visualise the outcomes of the experimental campaign outlined in the previous sections. The comparison is done based on changes in sample height throughout the F-T cycles as well as frost heave. Furthermore, it examined how the different layers of the samples change and whether they react the same way to the F-T cycles. Analysing any similarities, differences or discrepancies in them can reveal trends, patterns, or anomalies in the data. Additionally, methodological strengths and weaknesses, as well as knowledge gaps may be highlighted.

6. Experimental Campaign

6.1. Characterisation of the Mixtures

The experimental campaign can be divided into two stages. The first one consists of setting up the experiments by preparing the materials for the samples and determining the information required to characterise them. The type of clay used for the mixture was kaolin Speswhite and the type of sand was initially going to be Fontaiblean sand. However, not enough of this sand was available, therefore sand with similar grain size distribution had to be collected through sieving of other sand in order to replicate the characteristics of the Fontainebleau sand. Following the sieving process using the apparatus depicted in Figure 6.1, the obtained sand exhibited the grain size distribution illustrated in Figure 6.2. By comparing it to the curve of Fontainebleau sand obtained from Cabrillac et al. (2006), it can be seen that the used sand is not a perfect replacement for Fontainebleau sand and it is coarser compared to it. However, the distribution curve follows the same trend and it is close enough to assume that the used sand will have similar properties to Fontainebleau sand.

Figure 6.1: Sieving apparatus used for the grain size distribution
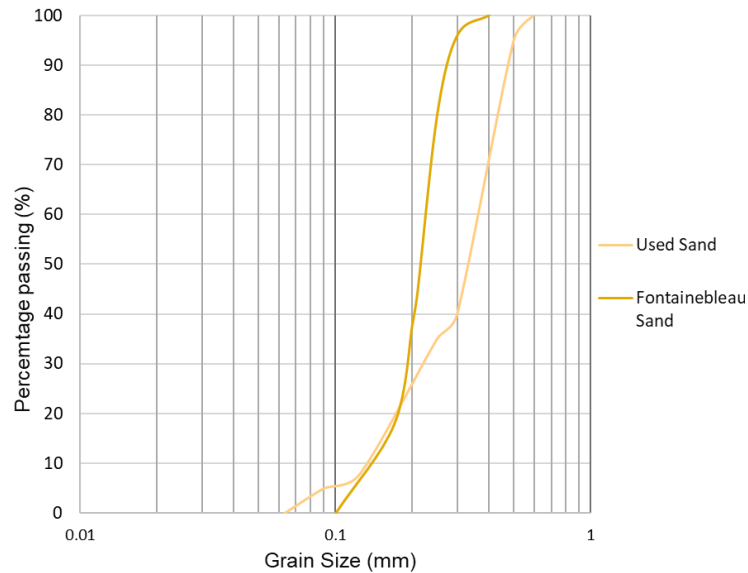
Figure 6.2: Grain size distribution of the used sand vs Fontainebleau sand

Following the preparation of the sand, the six soil mixtures introduced in Chapter 5 with fine contents of 5%, 10%, 20%, 50%, 60% and 70% were created and characterised. The soil mixtures were prepared by simply mixing sand and kaolin under completely dry conditions. The desired ratios between the two soil components were achieved by carefully weighing their contents before mixing. From here on, the mixtures will be referred to as Sx/Ky to indicate the sand content as x% and the kaolin content as y%. Therefore, a sample labelled S95/K05 means that the fine content equals 5% of the total sample weight and that the sand is 95% of the total weight.

As mentioned, the samples were stored and tested in transparent cylinders with an inner diameter of 3 cm and a height of around 6 cm. The maximum void ratio (e_{max}) was then found by filling the cylindrical containers to the top with the soil samples in a loose state, which gives its maximum volume (loose volume), hence the maximum void ratio. Following that, the soil samples were compacted by placing the containers with loose soil on the vibrating sieving apparatus shown in Figure 6.1 for 3 minutes. The soil particles rearranged due to the vibration and the volume of the soil decreased. After several vibration cycles, the volume stabilised and stopped decreasing (dense volume), thus the minimum void ratio (e_{min}) was achieved. By measuring the new sample height, the compacted volume is easily calculated. To derive the max and min void ratios, Equations 2 to 4 are utilised. The needed volume of solid particles in Equation 3 was calculated by weighing each sample separately and then subtracting the weight of the cylinders to get the mass only of the soil. Moreover, for the mixtures, the density of the solids that was used was 2.6 g/cm^3. This density was determined by taking the weighted average from the densities of the two soil components. However, since both kaolin Speswhite and Fontainebleau sand have a density of 2.6 g/cm^3, the weighted average value is 2.6 for all mixtures. The density of Fontainebleau sand and kaolin can be determined using their specific gravities and Equation 7. The specific gravity of the kaolin is equal to 2.6 (Thorel & Caicedo, 2015). The specific gravity of the used sand is between 2.6 and 2.65. The value of 2.6 was used in order to simplify calculations. Thus, the density of the two soil components is:

$$G_s = \frac{\rho_s}{\rho_w} \Rightarrow \rho_s = 2.6 * 1 = 2.6 g/cm^3 \qquad\qquad \textit{Equation 7}$$

Where:

- G_s - specific gravity [-]
- ρ_s - density of solids [g/cm^3]
- ρ_w - density of water [g/cm^3]

Knowing these parameters e_{max} and e_{min} are calculated and can be seen in Figure 6.3. It should be noted that the mixtures were tested three times to get more accurate results and the values presented in the figure are the average values of these three trials. All the information needed for the equations above that were used to obtain the figure is given in Appendix A. As expected, due to a greater number of voids the void ratio increases with higher clay content. This observation can also be supported by literature such as Kaothon et al. (2022) which state that an increase in fines causes an increase in both void ratio and compression index. Moreover, it is interesting to note that at low kaolin content, the change in void ratio between different mixtures is small. However, at higher kaolin percentages, the void ratio increases significantly with each mixture as presented in Figure 6.3.
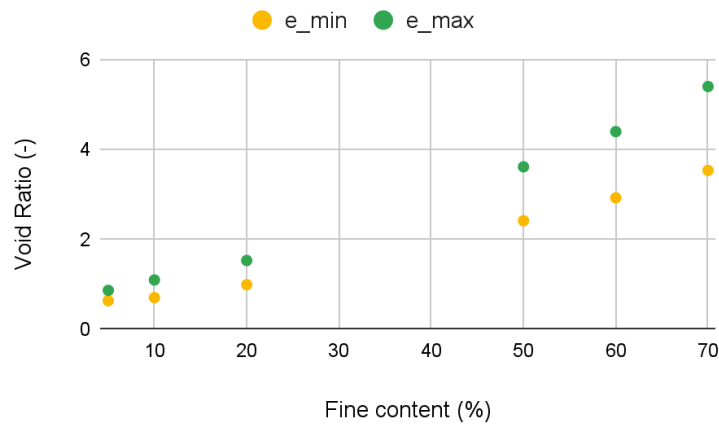
Figure 6.3: Min and max void ratios

The mixtures are also characterised based on their angle of repose. The value of the angle of repose can vary significantly depending on the method of measurement (Beakawi Al-Hashemi & Baghabra Al-Amoudi, 2018). The introduced in Chapter 5 funnel method is what is used in this study. For determining the angle of repose, 100 grams of each sample were prepared. A constant drop height of 5 cm between the bottom of the funnel and the top of the accumulated pile was chosen. The funnel had to be raised constantly to keep this 5 cm distance until all 100 grams were poured, at which point measurements of the height and diameter of the pile were taken. The setup for the experiment can be seen in Figure 6.4 and Figure 6.5.

Figure 6.6: Funnel method setup
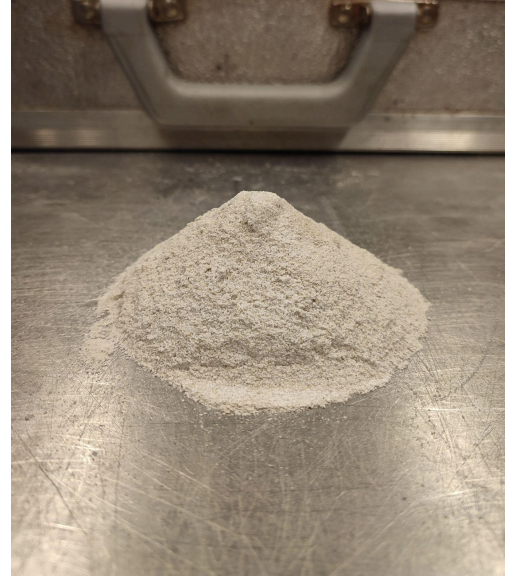
Figure 6.5: Pile formed by S50/K50

The experiment was again conducted three times for each mixture, and the angle of repose was calculated using Equation 1 each time to ensure reliability and prevent inaccurate results due to measurement errors. The average values from the results are presented in Table 6.1. Similar to the void ratio, when the mixture consists mostly of sand it has a lower repose angle. This can attributed to the increased surface area-to-volume ratio of smaller particles, resulting in greater friction and enhanced cohesion. This helps the particles to resist sliding, ultimately contributing to larger angles of repose.

Table 6.1: Angle of repose

Mixture	Height of pile (cm)	Diameter of pile (cm)	Repose angle (°)
S95/K05	2.35	9.6	26.08
S90/K10	2.93	9.37	32.06
S80/K20	3.6	10.43	34.62
S50/K50	4.9	12.53	38
S40/K60	5.2	13.47	38.04
S30/K70	5.6	12.43	42.01

To better visualize the increase in the angle of repose with a higher fine percentage, Figure 6.6 has been created.
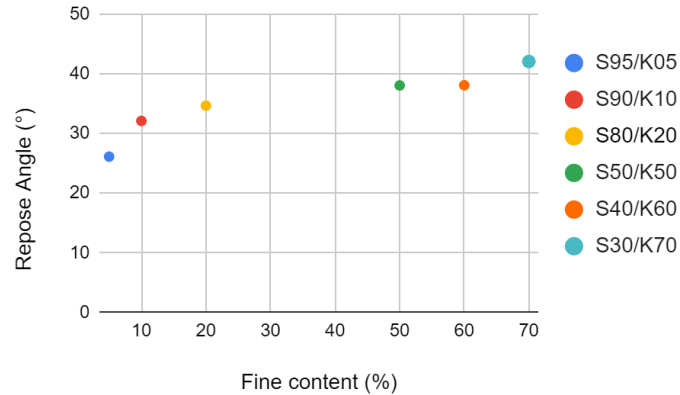
Figure 6.6: Repose angle vs fines

6.2. Testing the Samples

The second stage of the experimental campaign includes creating the samples and subjecting them to the freeze-thaw cycles. Similar to before, the experimental process was done three times per mixture. The samples were tested in three batches of 6 samples, one for each mixture. The soil samples were also tested in the same transparent cylinders used to determine e_{max} and e_{min}. However, in this instance, the cylindrical containers were filled with the soil mixtures only up to a height of 3 cm. This leaves space for water which is essential for the occurrence of heave and ensures that all samples have the same volume in the initial stage of the experiment, which will in turn foster a more meaningful and comparable analysis. Furthermore, the cylinders were filled with the soil mixtures in a dry loose state. The dry mass of the samples was mostly similar per mixture for the different batches. However, variations in the mass of a mixture, such as observed with the S50/K50 mixture - where the sample mass in the first trial was 12.9 g, compared to 15.84 g and 15.58 g in the second and third trials, respectively - could have been caused by the kaolin not being completely dry before mixing or inadvertent compaction while pouring them into the cylinders. Following that, the dry void ratios of the samples were calculated. They were determined by applying the same method as for e_{max} and e_{min}. The various variables, such as the mass, height and volume of solids of the samples, used to get the dry void ratio (e_{dry}) are shown in <u>Appendix B</u>. It should be noted that the volume of solids was calculated by imputing the dry mass of the samples in <u>Equation 3</u> and the same volumes of solids will be used to determine all void ratios throughout the experiments.

The samples were then saturated by immersion inside a vacuum bell (see <u>Figure 6.7</u>) to avoid the formation of air bubbles inside the samples. The samples were kept inside the bell for 20 hours to allow the water to be evenly distributed throughout. For 4 of these 20 hours, an air pump was used to create a vacuum by extracting all the air from the samples, thereby replacing the air in all the pores with water and fully saturating the samples. Given that the samples are 3 cm in height, the water level inside the vacuum bell was set at 4 cm above the bottom of the cylindrical containers. This setup guarantees sufficient water seepage through the bottom of the soil, causing the water film inside the containers to rise at least 1 cm above the top of the soil. During the de-airing process, all samples experienced a reduction in height, particularly those with higher kaolin percentages. Consequently, some samples exhibited a water film greater than 1 cm, while others had a water film below 1 cm. To address this discrepancy, it was determined that for the former, the water film would remain unchanged, whereas for the latter, additional

water was added to increase the film to 1 cm. This way it was ensured that enough water would be present for frost heave to occur during the second freezing. Additionally, after the saturation the bottom openings of the cylindrical containers are sealed with adhesive aluminium foil and teflon tape for pipes to prevent any loss of water and soil during the experiments.
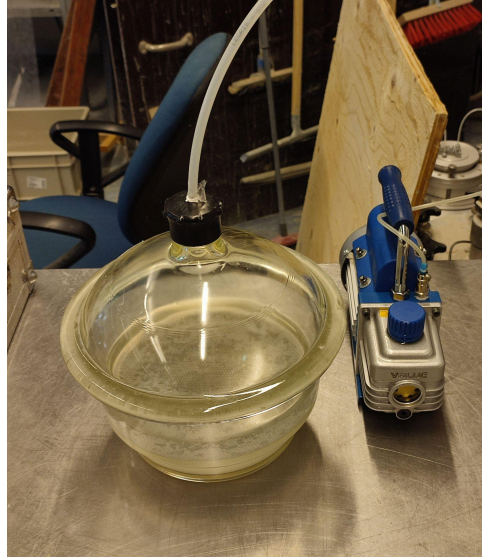

Figure 6.7: Vacuum bell used for the saturation and de-airing of the samples

After the saturation was completed, the changes in height and volume of each sample were recorded and are given in Appendix B. With that, the void ratios of the sample after saturation were estimated. The changes between the dry and saturated void ratio can be seen in Figure 6.8. The e_{dry} is significantly higher than e_{sat}, especially for the finer mixtures. Furthermore, the dry void ratio has values between e_{max} and e_{min}, whereas the saturated void ratio is much lower. This is due to the already mentioned significant collapses in the height of the samples during saturation. Since the height of the samples S50/K50, S40/K60, and S30/K70 decreased the most, their saturated void ratios are only slightly higher than that of the samples with mostly sand. Still, with higher clay content the void ratio increased which was mainly due to the lower mass of the three samples mentioned above, which resulted in a lower volume of solids.
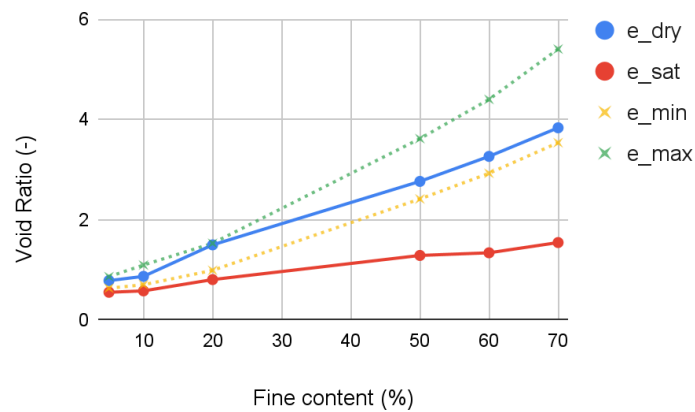
Figure 6.8: Void ratio vs fines

Following that, the de-aired samples were put in a standard freezer for 18 hours. For that, the cylinders were wrapped with the armaflex insulation as explained in <u>Chapter 5</u> to simulate real-world conditions in which the freezing of soil happens only from the top. After the freezing was carried out, the samples were removed from the freezer and left to thaw at room temperature for 4 hours. Then the same procedure of freezing and thawing was repeated one more time for the second and third batches of samples. For the first batch of samples, however, due to time constraints, the samples were subjected to freezing and thawing only once. After every freezing and thawing process, the change in sample height as well as the change in the height of the water film was noted and used to calculate the new void ratios, heave and water absorption. The results from the F-T cycles are discussed in detail in the next chapter.

7. Results

This chapter is divided into two sections. The first section examines the experimental findings and analyses them based on the research questions and research methods. The second section focuses on the comparative analysis of the results, with a detailed focus on frost heave behaviour and sample height changes.

7.1. Results from Experiments

7.1.1. Void Ratio

As discussed in the methodology chapter, understanding the void ratio changes during each stage of the experiments is crucial, as it directly affects frost heave. By utilising the already thoroughly explained method for void ratio calculation and measuring the sample height changes after every freezing and thawing process, Figures 7.1 to 7.6 are created. Appendix C contains all the output information from the experiments necessary to obtain the figures. The "X" in the annotation S95/K05_X shows from which test trial the results were derived. From the figures it is evident that the results vary for each batch of samples but still follow the same trends. During the freezing processes, the void ratio increased in all cases, or at least stayed the same for S95/K05, due to the expansion of the ice. Then it decreased once again during the two thawing periods. For the finer mixture, these changes in void ratio were more prominent. Still, the magnitude of change in the void ratio per mixture was similar between the first and second F-T cycles, however, the second F-T cycle (F2-T2) resulted in slightly lower void ratios for all mixtures. This also corresponds to observations made by Konrad and Lemieux (2005) that successive freeze-thaw cycles caused additional consolidation and a decrease in void ratio, as well as findings by Chamberlain and Gow (1979) that freezing and thawing always cause a decline in void ratio.

Furthermore, there are noticeable differences between the different batches of samples. The samples with lower percentages of clay have more similarities between the results from their second and third trials. On the other hand, the ones with higher clay content are quite different for all three trials. A possible explanation for this could be the difference between the dry masses of the three batches for some of the samples such as S90/K10 and S50/K50, and the different height reduction after saturation for other samples - S95/K05. Poor mixing during the preparation process could have caused incomplete blending of the sand and kaolin, leading to these discrepancies. Moreover, the results showcase that S40/K60 and S30/K70 mixtures exhibit unpredictable behaviour with significant variation in their responses to freezing and thawing.
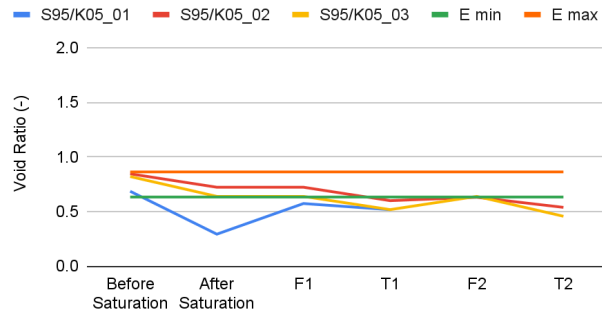
S95/K05

Figure 7.1: Void ratio S95/K05

S90/K10
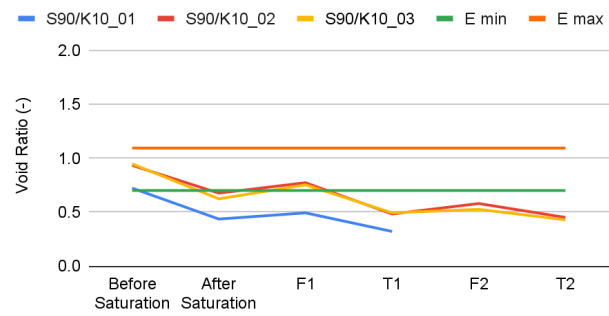
Figure 7.2: Void ratio S90/K10
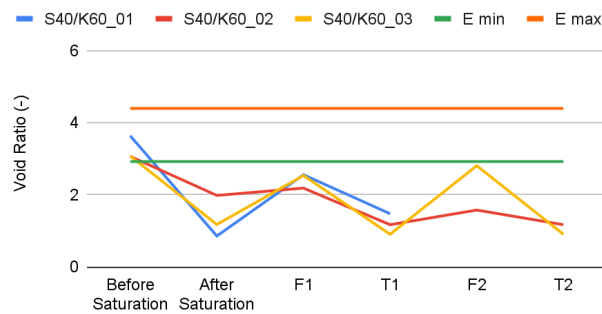
S80/K20
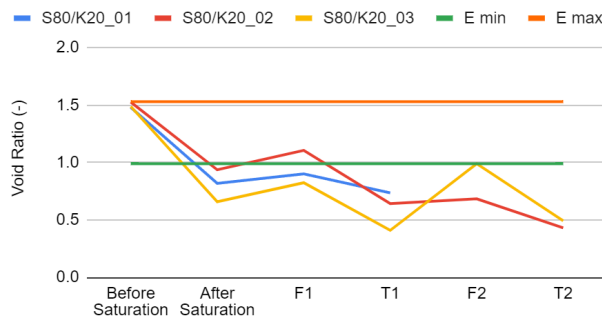
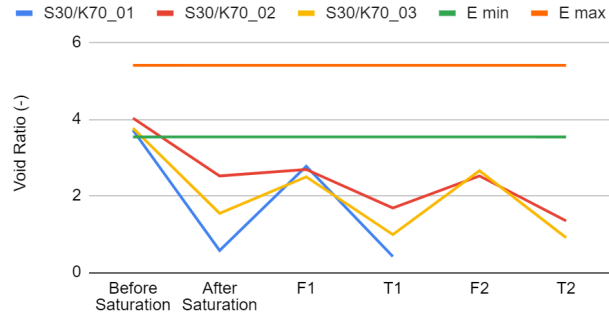*Figure 7.3: Void ratio S80/K20*

S50/K50
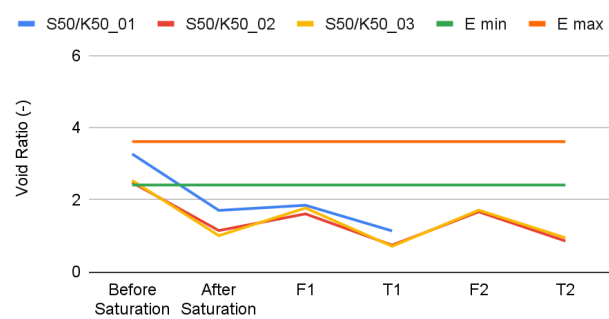
Figure 7.4: Void ratio S50/K50

S40/K60

Figure 7.5: Void ratio S40/K60

S30/K70

Figure 7.6: Void ratio S30/K70

Figure 7.7 shows the combined void ratio for the three test trials and its evolution throughout the experiments with respect to the fine content. This gives another perspective on the void ratio findings. It is clear that the void ratios during freezing (e_F1 and e_F2) are higher. The average content of voids is also very similar between the two freezing and two thawing processes, indicating that consecutive F-T cycles cause only a small further variation in the void ratio changes. Providing that the soil was subjected to more cycles, the outcome might have been different. Additionally, since the coarser mixtures contain fewer pores, less water can be retained within the soil, thereby decreasing heave and the subsequent

reduction in sample volume. Therefore, with less sand in the mixtures, the difference between the void ratio during freezing and during thawing increases significantly.
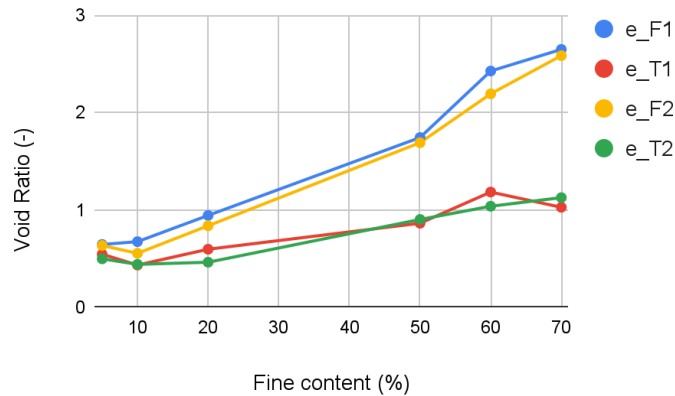
Figure 7.7: Combined void ratio

7.1.2. Frost Heave

Along with the void ratio, the frost heave findings are a crucial aspect of this study. This section examines these findings in detail. As explained in the research methods, the frost heave is measured using the frost heave ratio, as defined by Equation 5. The results are presented through three different types of graphs to enhance flexibility in analysis and provide a more comprehensive understanding of the soil's characteristics and behaviour.

The first three plots (Figure 7.8 to Figure 7.10) show how the frost heave develops after each freezing process. For the first trial, only the heave from the initial freezing (F1) is shown, as the samples underwent only one freezing cycle. Overall, from these figures, it can be observed that for the three mixtures with high sand content, the heave is lower compared to the other three mixtures. Two outliers for these three mixtures can be seen however, one for the first heave ratio of S95/K05 from the 1st trial and one for the second heave ratio of S80/K20 from the 3rd trial. The sample S95/K05 experienced this variation in the heave due to a more significant collapse after saturation in the first trial. For the S80/K20 mixture, the higher heave can be explained by the formation of a huge air cavity during T1 which can be seen in Figure 12.11 in Appendix E. For the three finer samples it is also noticeable that in the first trial the heave was considerably higher even though the samples' height after F1 was similar for all 3 trials. This is attributed to the greater decrease in height after saturation of the samples in the first batch. Moreover, the deviation in F2 heave between the 2nd and 3rd trials was most likely caused by the segregation that occurred in the fine mixtures from the last batch (see Figure 12.12 to Figure 12.17 in Appendix E). Another contributing factor is the fluctuation in water height, which occurred due to evaporation and insufficient sealing of the bottom of the cylinders, resulting in water leakage. The water level variability can be seen in Appendix D. Additionally, it should be noted that the soil heaved more during F2 compared to F1.
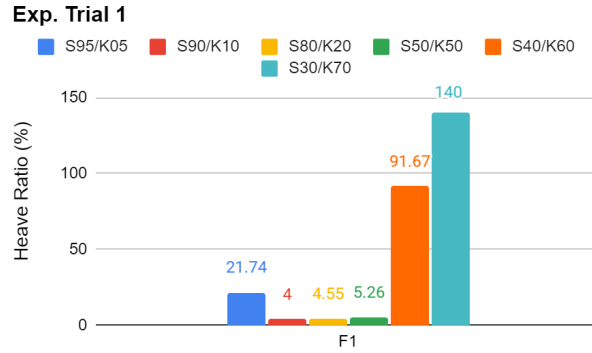
Figure 7.8: Frost heave for 1st batch of samples
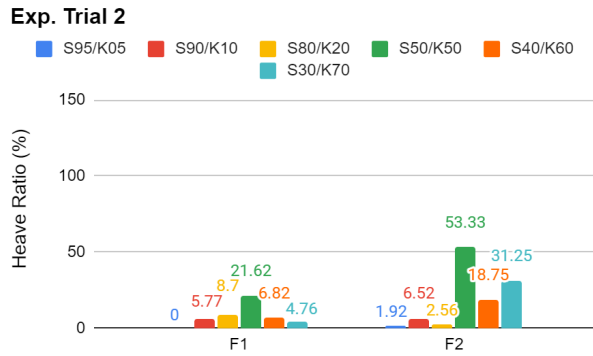
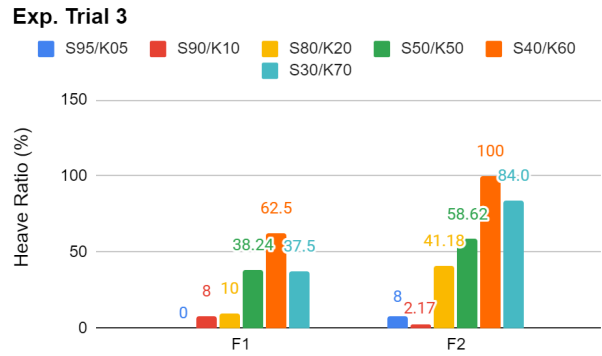*Figure 7.9: Frost heave for 2nd batch of samples*

Figure 7.10: Frost heave for 3rd batch of samples

Figure 7.11 serves as another way to present the heave ratio information. It is clear that on average the samples expand more during freezing with rising clay content. The difference between the 1st and 2nd heave is mostly equal for the various mixtures. The sole exception is the S50/K50 sample. A potential poor mixing or the already mentioned difference in weight of the sample in the three trials is the reason for this anomaly. Since the figure below only shows the average heave, more detailed plots are given in Appendix D.
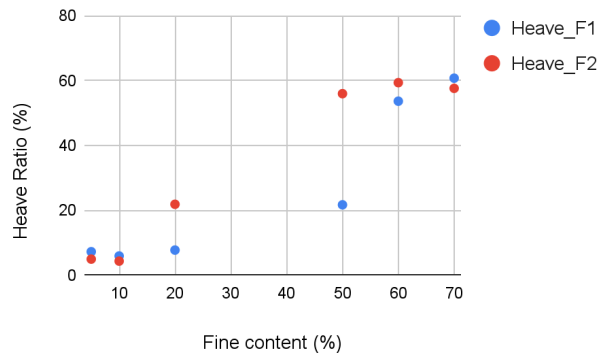
Figure 7.11: Average heave ratio vs fines

The average heave ratio of the samples is also plotted against the average void ratio with added standard deviation. From the figures below it can be seen that although the second heave is higher than the first,

they share a similar trend - the heave increases with a higher void ratio. In addition, increasing the void ratio also results in a more pronounced variation in the heave.
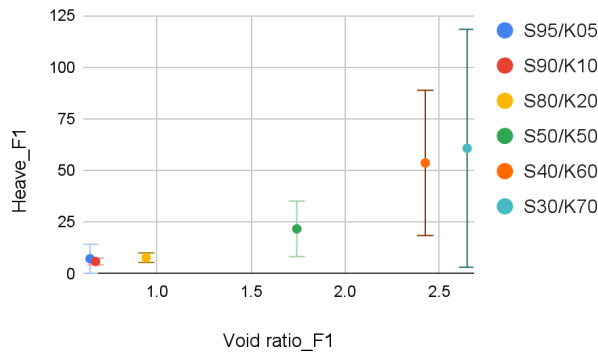
Figure 7.12: Frost heave vs void ratio 1st cycle
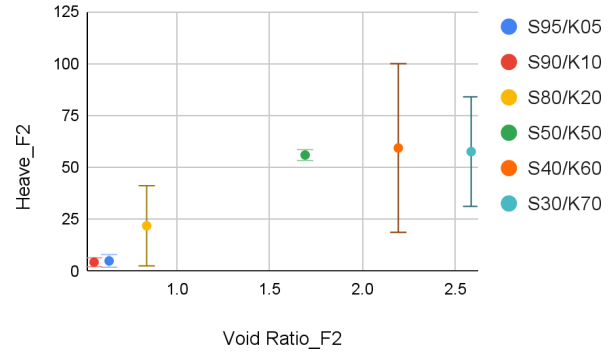
Figure 7.13: Frost heave vs void ratio 2nd cycle

7.1.3. Water Absorption

From the water film changes in Appendix D the water absorbed by the soil during freezing is determined. The absorption is measured by the decrease in the volume of water on top of the soil. Based on the three plots below, the soil absorbed more water the second time it was being frozen. The water volume was also reduced more during the second freezing. Another noticeable distinction between the results is the considerably higher absorption observed in the third trial. However, this is mostly due to the already-mentioned loss of water which magnifies the results. There is also a dependency between the absorption and the percentage of fines. The mixtures containing more kaolin seem to have absorbed higher amounts of the water film, likely because of their higher void ratio. The presence of more pores helped the soil in these samples to hold and absorb more water. Figure 12.10 in Appendix D compares the frequency of water absorption values across the three trials.
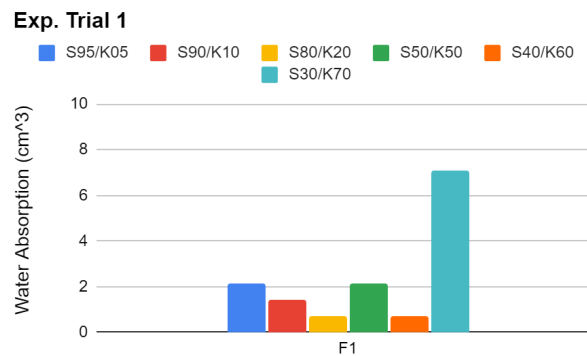
Figure 7.14: Water absorption for 1st batch of samples
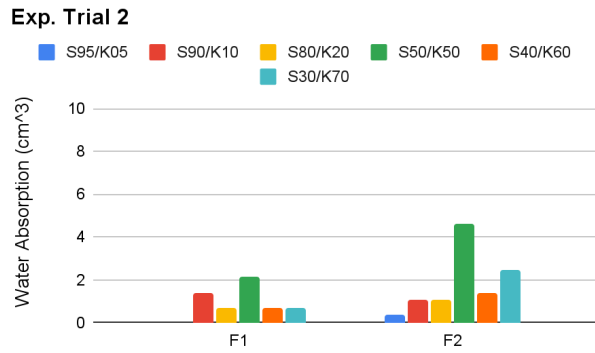
*Figure 7.15: Water absorption for 2nd batch of samples*   *Figure 7.16: Water absorption for 3rd batch of samples*
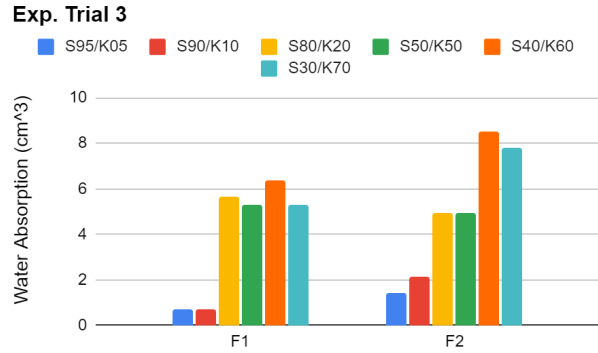
## 7.1.4. Segregation and Collapses in the Soil

Finally, the results from the experiments are analysed in terms of segregation and collapse during the F-T cycles. As previously discussed, in the last batch of samples, after saturation, different layers formed in the samples - one with high percentages of kaolin on top and one with predominantly sand on the bottom of the samples. This segregation together with the already mentioned air bubble in the third S80/K20 sample can be seen in Appendix E. Furthermore, the microstructure of the soils is also observed for other forms of segregation such as the formation of ice lenses. After every thaw-freeze cycle ice lenses developed in all samples and can be seen in Appendix E as well. In the S95/K05 and S90/K10 these ice lenses are hardly visible, as depicted in Figures 12.18 and 12.19. However, with every increase in the kaolin content, the lenses become more prominent. Ultimately, an increased number of pores in the soil enhances water migration, thereby facilitating the formation of ice lenses. Interestingly, the ice lenses did not form horizontally as expected but rather vertically or irregularly. Possible reasons for this include the fact that the freezing of the samples was not strictly one-dimensional from the top. Even though the samples were wrapped with insulation material, the freezing temperatures in the freezer affected the soil laterally as well. In Figures 7.17 to 7.20, four examples of the ice lenses are given.
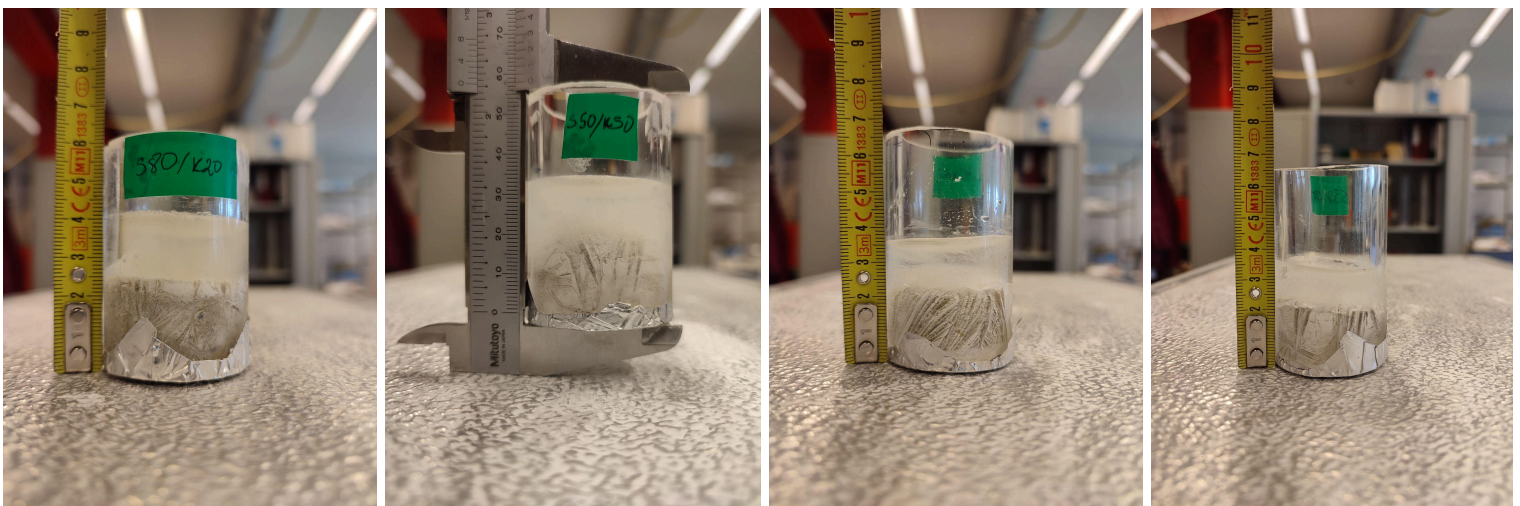
Figures 7.17, 7.18, 7.19 & 7.20: Samples S80/K20_02, S50/K50_02, S40/K60_02 and S40/K70_02 after F1

The only sample in which the ice lenses developed horizontally was the S40/K60 mixture from the third batch. After it was frozen the first time, the ice lenses evolved as previously expected, however, after the thawing and subsequent second freezing, they changed their orientation.
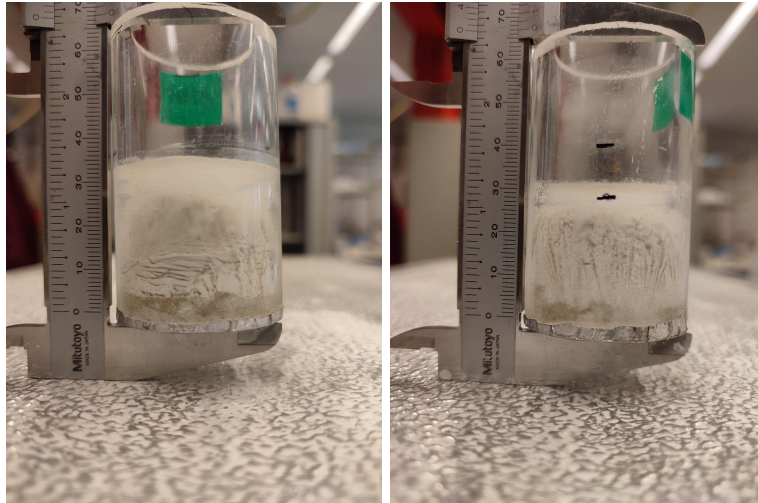

Figures 7.21 & 7.22: Samples S40/K60_03 after F1 and S40/K60_03 after F2

No other sign of collapses or soil segregation can be seen in the samples without the use of specific equipment or methods such as X-ray tomography.

7.2. Comparison to Previous Results

In this final section, the experimental findings are contrasted with outcomes from an earlier study. These previous outcomes are in the form of 3D scans made with X-ray tomography. Using the Fiji image processing tool the data from these scans is extracted. A more detailed overview of this tool is shown in Appendix F. Data only about the S95/K05, S90/K10, S80/K20 and S50/K50 mixtures are present from the previous study.

First, the change in sample height is compared - see Figure 7.23 to Figure 7.26. Although initially, the estimated sample height from the experiments corresponds to that of the previous study, after subjecting the soil to the F-T cycle considerable variation in height occurs. In all four instances that is due to a much greater increase of the height after the first freezing. Another difference is that the change in height of the comparative samples is of a greater magnitude for all stages. Even though this variation greatly contrasts the two results, the sample height follows the same trend in both cases. The values from the previous results of the S50/K50 mixture are the only exception to that and have a weird evolution due to segregation and air bubbles that had formed in that sample.

S95/K05
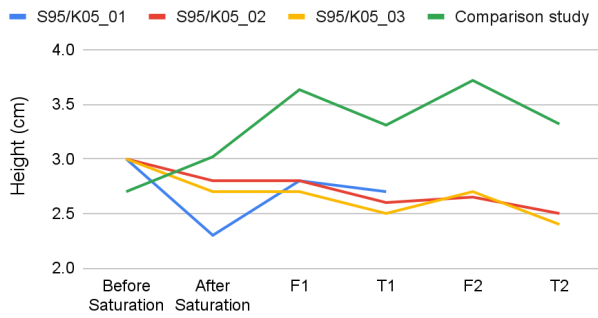
Figure 7.23: Sample height S95/K05

S90/K10
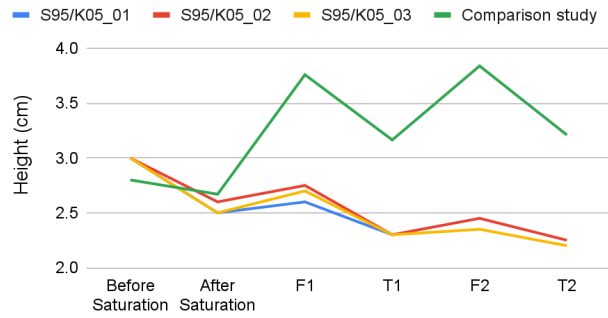
Figure 7.24: Sample height S90/K10

S80/K20
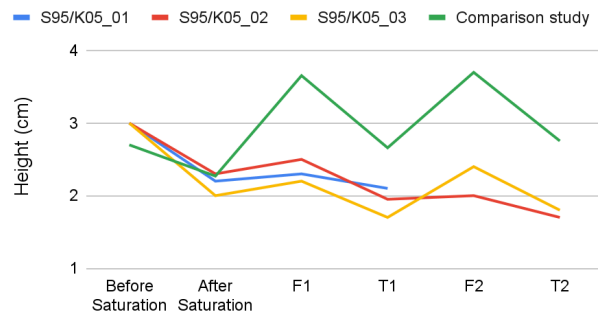
Figure 7.25: Sample height S80/K20

S50/K50
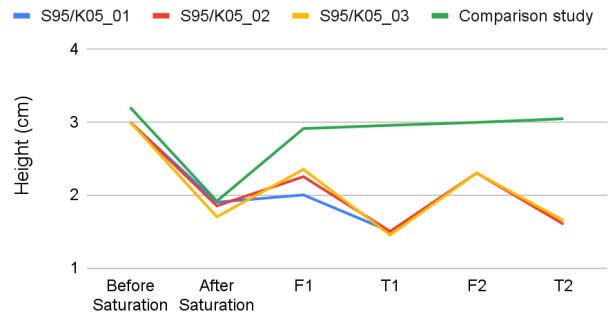
Figure 7.26: Sample height S50/K50

Knowing the height changes, the heave ratio from the other study can also be calculated and compared to the results from <u>Section 7.1.2</u>. At the first freezing, the samples in the experimental campaign heaved a lot less than in the comparative study, especially for the coarser mixtures. This significant difference can be explained by the loss of water in some of the samples in the conducted experiments During F2, however, the situation was very similar between the two results. Overall, the sample height and heave outcomes are not that different from those of the previous experiment. Furthermore, any major discrepancies in the results can also be attributed to a different method of mixing the samples, since it is not known how the samples in the comparative study were prepared. Given that the samples in the other study underwent 1-dimensional freezing from the bottom with a freezing plate, the ice lenses in those samples likely formed horizontally. This difference in ice lens formation potentially contributed to the disparities in heave observed between the studies. However, it is not known how significant the impact of this is.
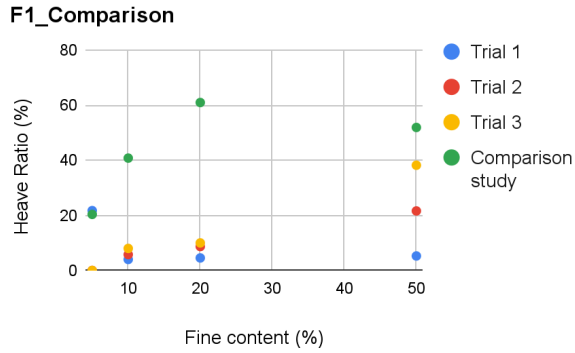
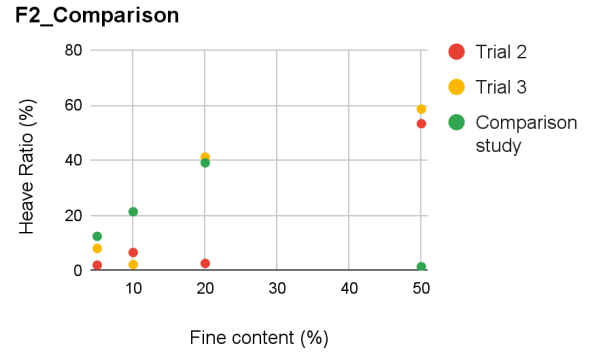*Figure 7.27: Average heave for 1st freezing*

Figure 7.28: Average heave for 2nd freezing

To further understand how the soil mixtures behave during freezing and thawing, it is analysed which layers of the soil are affected the most by the F-T cycles. The samples used in the comparative study each contained five tracers (glass ballotini) positioned vertically above one another. These tracers were employed to track the volume deformations faster. To determine if the upper layers of the samples experience more heave, the tracer displacement is plotted. The following figures present the z-coordinate changes, i.e. vertical displacement, of the tracers for the different steps of the experiment. As explained in Appendix F, 00S is the state of the samples after saturation, 03S is the samples after the completion of the first freezing process, 05S is the samples after the first thawing, while 08S corresponds to F2 and 10S to T2. Based on the figures, the tracers in the upper layers change their vertical positioning more relative to the tracers in the bottom of the cylinders. Meaning that the top of the samples does indeed heave more. This, however, is to be expected since the formation of the ice lenses happens in the middle and top of the soil, thus pushing the top layers of the soil upwards.
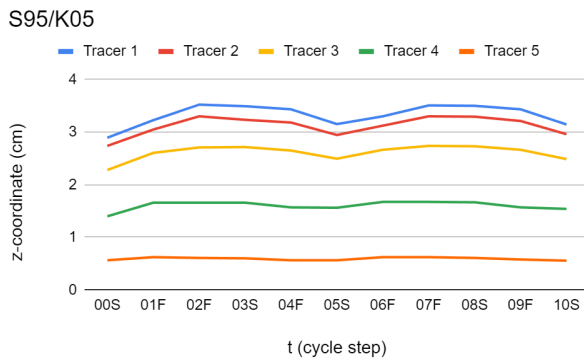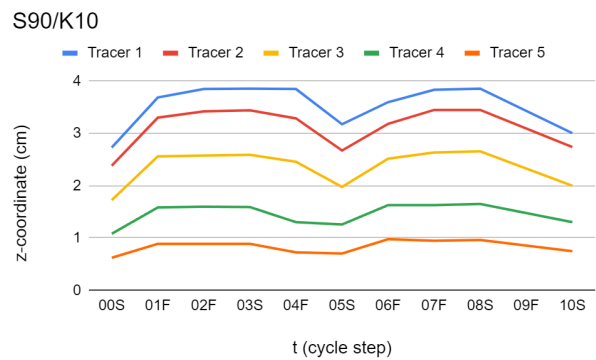

Figure 7.29: Tracers height S95/K05
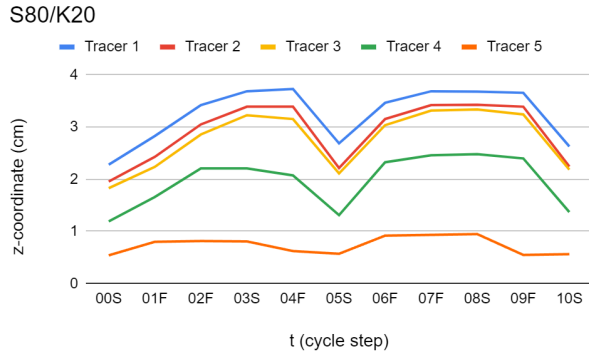

Figure 7.30: Tracers height S90/K10

Figure 7.31: Tracers height S80/K20

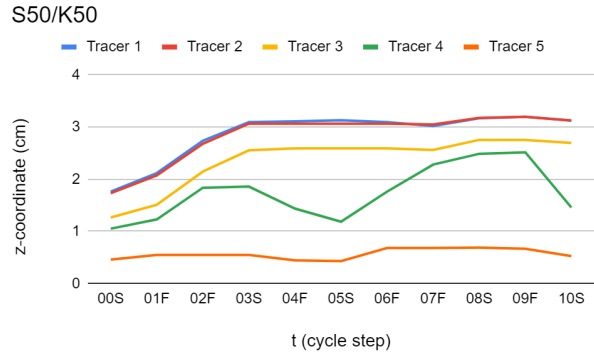Figure 7.32: Tracers height S50/K50

The horizontal displacement of the tracers was also plotted and can be found in Appendix F. It was determined that freezing and thawing do not have a significant effect on horizontal displacement of the tracers. Furthermore, 3D plots are created using python to visualise the change in the position of the tracers simultaneously in all directions. The plots showing this are provided in Figures 12.30 to 12.33 in Appendix F. From the analysis of these plots it can be determined that the deformations in the soil are only significant along the z-axis, whereas the lateral deformations are negligible.

8. Discussion

The experimental campaign and the results from it showed that sand-clay soils are indeed heavily affected by freeze-thaw cycles. However, it was established that many other aspects can also influence the reaction of the soil to these cycles in an experimental setting. Nonetheless, the results still closely represent reality. For instance, with a higher percentage of kaolin in the mixtures, the void ratio increased as anticipated. The mass of the samples also decreased with more kaolin, indicating a rise in the number of pore spaces due to the finer particles. Additionally, it was determined that the water absorption and consequently the heave ratio also grow when the sand particles in the mixtures are less. Accordingly, it can be inferred that further increasing the kaolin content will result in even lighter and more porous samples that exhibit greater volume expansion during freezing. This is also further supported by the conducted comparison. Although the results from the experiments and the previous study are not entirely similar they follow the same trends, thus highlighting the accuracy of the findings in this report.

Nevertheless, the results also revealed some anomalies and unexpected findings. After plotting the frost heave development, some discrepancies were observed between the results from the three experimental trials. These variations were attributed to the sample compaction after saturation and differing water absorption in the three batches. However, it is more likely that these inconsistencies were caused by water loss and insufficient mixing of the sand and clay in some samples, rather than the inherent soil properties. Moreover, even with insulation, freezing the samples from all sides led to the ice unexpectedly forming both horizontally and vertically.

Overall, the results from this study are close to reality and manage to advance the understanding of soil behaviour under freezing and thawing conditions. However, not all aspects of the soil behaviour were studied in this work. In future research, other qualities of the soil mixtures can be further examined. Some such qualities can be the changes in the density of the samples and the pore distribution of the mixtures. Furthermore, conducting more trials or subjecting the samples to more F-T cycles could provide more accurate results and contribute to a broader comprehension of the soil properties.

9. Conclusion

In conclusion, the research objective to expand the understanding of the volumetric behaviour of sand and clay mixtures under freeze-thaw cycles was achieved. The aims of this report were met through the experimental campaign and subsequent analysis and comparison of the results. Six sand-clay samples were tested with kaolin contents of 5%, 10%, 20%, 50%, 60% and 70%, respectively. Through characterising them it was determined that the min and max void ratio and repose angle have higher values for the mixtures containing more kaolin. After testing the samples, this trend with the void ratio continued for every stage of the experiments, ranging from values around 0.6 for S95/K05 to 2.7 for S30/K70. In addition, as the void ratio increased, so did the variation in its values.

Furthermore, subjecting the mixtures to the same experimental procedure lead to different outcomes for the samples from the 6 mixtures. The samples with more kaolin prove to be more susceptible to both saturation and freeze-thaw cycles. The analysis also determined that the frost heave during the second cycle was up to 2 times higher than during the first cycle. This, however, was for the finer mixtures, while the coarser mixtures experienced only a slight increase in the heave. Similarly, when segregation and collapses occurred in some of the batches, it was always in the samples comprising of high percentages of clay. Several factors related to both the soil properties and experimental procedure have been pointed out as a reason for these findings, e.g. the different cohesiveness and porosities of the mixtures as well as human error while mixing and sealing the samples. Other factors such as the irregular formation of the ice lenses are considered to be less significant. Vertically oriented ice lenses still fill the pore spaces and cause soil expansion. Moreover, it is harder to determine the exact impact that the change in their orientation has on the outcomes. Following a comparison of the experimental observations to previously obtained results from another study, it was concluded that the outcomes of the experiment were satisfactory and close to reality. Using the results from the previous results, further analysis was conducted and it was found that the upper layers of the soil are more likely to rise during freezing.

To conclude, while this study deepens our understanding of soil behaviour under freeze-thaw cycles, it's important to acknowledge that several other soil properties influenced by these cycles were not taken into consideration in this research. Moreover, the findings were derived through an experimental campaign that, while aimed at representing reality, may not perfectly mirror real-world conditions.

10. Recommendations

This study extensively examined the reactions of soils to freezing and thawing. While most of the results aligned with expectations, there is still potential for further improvement. First, it is essential to prevent as many errors while conducting the experiments as possible. Following a strict procedure could help in achieving that. Additionally, conducting a preliminary test trial with just one or two samples can identify areas for improvement in the experimental campaign. However, human errors can always occur. Therefore, their effect on the results could be further minimised by more repetitions of the experiments, i.e. more experimental trials. More tests could also lead to lower uncertainties regarding the results. Secondly, the experimental procedure can be adjusted to better simulate reality by freezing the samples only one-dimensionally from the top. Lastly, future research could investigate a greater number of consecutive freeze-thaw cycles to determine if the soil continues to exhibit the same property changes after additional cycles.

11. References

Beakawi Al-Hashemi, H. M., & Baghabra Al-Amoudi, O. S. (2018). A review on the angle of repose of granular materials. *Powder Technology*, *330*, 397–417. https://doi.org/10.1016/j.powtec.2018.02.003

Benkelman, A. C., & Olmsetead, F. R. (1932). A New Theory Of Frost Heaving. *Highway Research Board Proceedings*, *11*, pp 165-177. https://onlinepubs.trb.org/Onlinepubs/hrbproceedings/11/11-029.pdf

Cabrillac, R., Djeran-Maigre, I., Delfosse-Ribay, E., & Gouvenot, D. (2006). Factors Affecting the Creep Behavior of Grouted Sand. *Journal of Geotechnical and Geoenvironmental Engineering*, *132*(4), 488–500. https://doi.org/10.1061/(ASCE)1090-0241(2006)132:4(488)

Chamberlain, E. J., & Gow, A. J. (1979, January 1). *Effect of Freezing and Thawing on the Permeability and Structure of Soils* (H. L. Jessberger, Ed.). ScienceDirect; Elsevier. https://www.sciencedirect.com/science/article/abs/pii/B9780444417824500129

Čejka, J., Roth, W., & Opanasenko, M. (2017). Two-Dimensional Silica-Based Inorganic Networks. *Comprehensive Supramolecular Chemistry II*, 475–501. https://doi.org/10.1016/B978-0-12-409547-2.13647-9

Das, B. M., & Sobhan, K. (2014). Principles of Geotechnical Engineering, SI 8th Edition. In *Google Books*. Cengage Learning. https://books.google.nl/books/about/Principles_of_Geotechnical_Engineering_S.html?id=L925C gAAQBAJ&redir_esc=y

Guoyu, L., Wei, M., Yanhu, M., & Zhou, C.-L. . (2011). Process and mechanism of impact of freezing and thawing cycle on collapse deformation of compacted loess. *Journal of Highway and Transport*, *24*(5). https://www.researchgate.net/publication/289792217_Process_and_mechanism_of_impact_of_fre ezing_and_thawing_cycle_on_collapse_deformation_of_compacted_loess

Hjort, J., Streletskiy, D., Doré, G., Wu, Q., Bjella, K., & Luoto, M. (2022). Impacts of permafrost degradation on infrastructure. *Nature Reviews Earth & Environment*, *3*(1), 24–38. https://doi.org/10.1038/s43017-021-00247-8

Huang, Y., Chen, Y., Wang, S., Wu, M., & Wang, W. (2022). Effects of Freeze-Thaw Cycles on Volume Change Behavior and Mechanical Properties of Expansive Clay with Different Degrees of Compaction. *International Journal of Geomechanics*, *22*(5). https://doi.org/10.1061/(ASCE)GM.1943-5622.0002347

Kaothon, P., Lee, S.-H., Choi, Y.-T., & Yune, C.-Y. (2022). The Effect of Fines Content on Compressional Behavior When Using Sand–Kaolinite Mixtures as Embankment Materials. *Applied Sciences*, *12*(12), 6050–6050. https://doi.org/10.3390/app12126050

Konrad, J.-M., & Lemieux, N. (2005). *Influence of fines on frost heave characteristics of a well-graded base-course material*. *42*(2), 515–527. https://doi.org/10.1139/t04-115

Lade, P. V., Yamamuro, J. A., & Liggio, C. D. Jr. (2009). Effects of fines content on void ratio, compressibility, and static liquefaction of silty sand. *Geomechanics and Engineering*, *1*(1), 1–15. https://doi.org/10.12989/gae.2009.1.1.001

Liu, J., Chang, D., & Yu, Q. (2016). Influence of freeze-thaw cycles on mechanical properties of a silty sand. *Engineering Geology*, *210*, 23–32. https://doi.org/10.1016/j.enggeo.2016.05.019

Lohner, S. (2019, February 14). *Slippery Slopes, and the Angle of Repose*. Scientific American. https://www.scientificamerican.com/article/slippery-slopes-and-the-angle-of-repose/

Nadeem Akhtar, M. (2012, September). *Role of Soil Mechanics In Civil Engineering*. Research Gate. https://www.researchgate.net/publication/261366087_Role_of_Soil_Mechanics_In_Civil_Engineering

Penner, E. (1959). The mechanism of frost heaving in soils. *Highway Research Board Bulletin*, *225*. https://trid.trb.org/view/128111

Phan, V. T.-A., Hsiao, D.-H., & Nguyen, P. T.-L. (2016). Effects of Fines Contents on Engineering Properties of Sand-Fines Mixtures. *Procedia Engineering*, *142*, 213–220. https://doi.org/10.1016/j.proeng.2016.02.034

Saetersdal, R. (1981). Heaving conditions by freezing of soils. *Engineering Geology*, *18*(1-4), 291–305. https://doi.org/10.1016/0013-7952(81)90068-5

She, W., Cao, X., Zhao, G., Cai, D., Jiang, J., & Hu, X. (2018). Experimental and numerical investigation of the effect of soil type and fineness on soil frost heave behavior. *Cold Regions Science and Technology*, *148*, 148–158. https://doi.org/10.1016/j.coldregions.2018.01.015

Thorel, L., & Caicedo, B. (2015). Effects of cracks and desiccation on the bearing capacity of soil deposits. *Géotechnique Letters*, *5* (July-September), 112–117. https://doi.org/10.1680/geolett.15.00021

Valves Instruments Plus Ltd. (n.d.). *Density Of Liquid Water From 0°C to 100°C*. https://www.vip-ltd.co.uk/Expansion/Density_Of_Water_Tables.pdf

Yin, K., Fauchille, A.-L., Di Filippo, E., Kotronis, P., & Sciarra, G. (2021). A Review of Sand–Clay Mixture and Soil–Structure Interface Direct Shear Test. *Geotechnics*, *1*(2), 260–306. https://doi.org/10.3390/geotechnics1020014

12. Appendices

12.1. Appendix A: Min and Max Void Ratio

As discussed in the report, the experiment was executed three times to evaluate the accuracy of the results. Table 12.1 shows the average values of the parameters for which e_{max} and e_{min} were derived, such as the volume of solids, and mass and height of samples. From the results, it can be seen that the finer samples compacted more and had a lower mass. This can be explained by the presence of more pores in these soil samples. Therefore, lower sand contents resulted in higher void ratios. Additionally, upon closer examination of the void ratio, it becomes evident that the difference between the maximum and minimum void ratio values grows for finer mixtures, as depicted in Figure 12.1. This occurs most likely due to the larger number of void spaces in the fine mixtures.

Table 12.1: Minimum and maximum void ratios

| Mixture	Height of loose soil (cm)	Height of dense soil (cm)	Mass of sample (g)	Volume of loose soil (cm³)	Volume of dense soil (cm³)	Volume of solid (cm³)	e_{max} (-)	e_{min} (-)
S95/K05	6.4	5.62	63.29	45.24	39.70	24.34	0.86	0.63
S90/K10	6.4	5.2	56.18	45.24	36.76	21.61	1.09	0.7
S80/K20	6.4	5.03	46.51	45.24	35.58	17.89	1.53	0.99
S50/K50	6.4	4.73	25.82	45.24	33.46	9.93	3.56	2.37
S40/K60	6.4	4.65	21.78	45.24	32.87	8.38	4.40	2.93
S30/K70	6.4	4.53	18.51	45.24	32.04	7.12	5.36	3.50
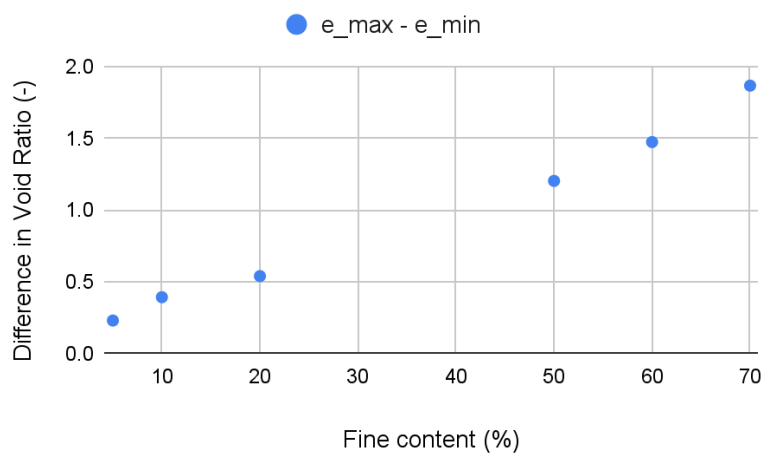
Figure 12.1: Difference between e_{max} and e_{min}

12.2. Appendix B: Void Ratio Before and After Saturation

The table below shows the data for both the dry and saturated void ratios for all three trials.

Table 12.2: Result from calculations for e_{dry} and e_{sat}

	After Saturation									
Sample	Mass of sample before saturation (g)	Mass of Sand (g)	Mass of kaolin (g)	Height of sample before saturation (cm)	Height of sample after saturation (cm)	Volume of sample before saturation (cm^3)	Volume of sample after saturation (cm^3)	Volume of solid (cm^3)	Void Ratio before saturation (-)	Void Ratio after saturation (-)
S95/K05_01	32.72	31.084	1.636	3	2.3	21.2058	16.2577	12.5846	0.6851	0.2919
S95/K05_02	29.88	28.386	1.494	3	2.8	21.2058	19.7920	11.4923	0.8452	0.7222
S95/K05_03	30.29	28.776	1.515	3	2.7	21.2058	19.0852	11.6500	0.8202	0.6382
S90/K10_01	32	28.8	3.2	3	2.5	21.2058	17.6715	12.3077	0.7230	0.43581
S90/K10_02	28.5	27.075	1.425	3	2.6	21.2058	18.3783	10.9615	0.9346	0.6766
S90/K10_03	28.3	26.885	1.415	3	2.5	21.2058	17.6715	10.8846	0.9482	0.6235
S80/K20_01	22.24	17.792	4.448	3	2.2	21.2058	15.5509	8.5538	1.4791	0.8180
S80/K20_02	21.83	17.464	4.366	3	2.3	21.2058	16.2577	8.3962	1.5257	0.9363
S80/K20_03	22.17	17.736	4.434	3	2	21.2058	14.1372	8.5269	1.4869	0.6579
S50/K50_01	12.9	6.450	6.450	3	1.9	21.2058	13.4303	4.9615	3.2740	1.7069
S50/K50_02	15.84	7.920	7.920	3	1.85	21.2058	13.0769	6.0923	2.4807	1.1465
S50/K50_03	15.58	7.790	7.790	3	1.7	21.2058	12.0166	5.9923	2.5388	1.0053
S40/K60_01	11.88	4.752	7.128	3	1.2	21.2058	8.4823	4.5692	3.6410	0.8564
S40/K60_02	13.55	5.420	8.130	3	2.2	21.2058	15.5509	5.2115	3.0690	1.9839
S40/K60_03	13.51	5.404	8.106	3	1.6	21.2058	11.3097	5.1962	3.0810	1.1766
S30/K70_01	11.7	3.510	8.190	3	1	21.2058	7.0686	4.5000	3.7124	0.5708
S30/K70_02	10.97	3.291	7.679	3	2.1	21.2058	14.8440	4.2192	4.0260	2.5182
S30/K70_03	11.57	3.471	8.099	3	1.6	21.2058	11.3097	4.4500	3.7653	1.5415

12.3. Appendix C: Results from F-T Cycles

The table below displays all the data obtained from the F-T cycles.

Table 12.3: Results from the F-T cycles

Sample	F-T cycle	Mass of sample (g)	Sample height after saturation (cm)	New sample height (cm)	New volume of sample (cm^3)	Initial water height (cm)	New water height (cm)	Water absorpted (cm^3)	Heave ratio (%)	Volume of solid (cm^3)	New void ratio (-)
					After Freezing and Thawing						
S95/K05_01	F1	32.72	2.3	2.8	19.7920	1	0.7	2.1206	21.7391	12.5846	0.5727
	T1	32.72	2.3	2.7	19.0852	1	0.5	-	-	12.5846	0.5165
S95/K05_02	F1	29.88	2.8	2.8	19.7920	1	1	0	0	11.4923	0.7222
	T1	29.88	2.8	2.6	18.3783	1	0.9	-	-	11.4923	0.5992
	F2	29.88	2.8	2.65	18.7317	1	0.85	0.3534	1.9231	11.4923	0.6299
	T2	29.88	2.8	2.5	17.6715	1	0.9	-	-	11.4923	0.5377
S95/K05_03	F1	30.29	2.7	2.7	19.0852	1	0.9	0.7069	0	11.65	0.6382
	T1	30.29	2.7	2.5	17.6715	1	1	-	-	11.65	0.5169
	F2	30.29	2.7	2.7	19.0852	1	0.8	1.4137	8	11.65	0.6382
	T2	30.29	2.7	2.4	16.9646	1	0.85	-	-	11.65	0.4562
S90/K10_01	F1	32	2.5	2.6	18.3783	1	0.8	1.4137	4	12.3077	0.4932
	T1	32	2.5	2.3	16.2577	1	1	-	-	12.3077	0.3209
S90/K10_02	F1	28.5	2.6	2.75	19.4386	1.2	1	1.4137	5.7692	10.9615	0.7733
	T1	28.5	2.6	2.3	16.2577	1.2	0.95	-	-	10.9615	0.4832
	F2	28.5	2.6	2.45	17.3180	1.2	0.8	1.0603	6.5217	10.9615	0.5799
	T2	28.5	2.6	2.25	15.9043	1.2	0.9	-	-	10.9615	0.4509
S90/K10_03	F1	28.3	2.5	2.7	19.0852	1.1	1	0.7069	8	10.8846	0.7534
	T1	28.3	2.5	2.3	16.2577	1.1	1	-	-	10.8846	0.4936
	F2	28.3	2.5	2.35	16.6112	1.1	0.7	2.1206	2.1739	10.8846	0.5261
	T2	28.3	2.5	2.2	15.5509	1.1	0.8	-	-	10.8846	0.4287
S80/K20_01	F1	22.24	2.2	2.3	16.2577	1.5	1.4	0.7069	4.5455	8.5538	0.9006
	T1	22.24	2.2	2.1	14.8440	1.5	1.5	-	-	8.5538	0.7354
S80/K20_02	F1	21.83	2.3	2.5	17.6715	1.5	1.4	0.7069	8.6957	8.3962	1.1047
	T1	21.83	2.3	1.95	13.7837	1.5	1.45	-	-	8.3962	0.6417
	F2	21.83	2.3	2	14.1372	1.5	1.3	1.0603	2.5641	8.3962	0.6838
	T2	21.83	2.3	1.7	12.0166	1.5	1.15	-	-	8.3962	0.4312
S80/K20_03	F1	22.17	2	2.2	15.5509	1.6	0.8	5.6549	10	8.5269	0.8237
	T1	22.17	2	1.7	12.0166	1.6	1	-	-	8.5269	0.4093
	F2	22.17	2	2.4	16.9646	1.6	0.3	4.9480	41.1765	8.5269	0.9895
	T2	22.17	2	1.8	12.7235	1.6	0.8	-	-	8.5269	0.4922
S50/K50_01	F1	12.9	1.9	2	14.1372	1.7	1.4	2.1206	5.2632	4.9615	1.8494
	T1	12.9	1.9	1.5	10.6029	1.7	2	-	-	4.9615	1.1370
S50/K50_02	F1	15.84	1.85	2.25	15.9043	1.8	1.5	2.1206	21.6216	6.0923	1.6106
	T1	15.84	1.85	1.5	10.6029	1.8	1	-	-	6.0923	0.7404
	F2	15.84	1.85	2.3	16.2577	1.8	0.35	4.5946	53.3333	6.0923	1.6686
	T2	15.84	1.85	1.6	11.3097	1.8	0.85	-	-	6.0923	0.8564
S50/K50_03	F1	15.58	1.7	2.35	16.6112	2.1	1.35	5.3014	38.2353	5.9923	1.7721
	T1	15.58	1.7	1.45	10.2494	2.1	1.2	-	-	5.9923	0.7104
	F2	15.58	1.7	2.3	16.2577	2.1	0.5	4.9480	58.6207	5.9923	1.7131
	T2	15.58	1.7	1.65	11.6632	2.1	1	-	-	5.9923	0.9464
S40/K60_01	F1	11.88	1.2	2.3	16.2577	1.1	1	0.7069	91.6667	4.5692	2.5581
	T1	11.88	1.2	1.6	11.3097	1.1	1.8	-	-	4.5692	1.4752
S40/K60_02	F1	13.55	2.2	2.35	16.6112	1.6	1.5	0.7069	6.8182	5.2115	2.1874
	T1	13.55	2.2	1.6	11.3097	1.6	2	-	-	5.2115	1.1701
	F2	13.55	2.2	1.9	13.4303	1.6	1.8	1.4137	18.75	5.2115	1.5770
	T2	13.55	2.2	1.6	11.3097	1.6	1.6	-	-	5.2115	1.1701
S40/K60_03	F1	13.51	1.6	2.6	18.3783	2.2	1.3	6.3617	62.5	5.1962	2.5369
	T1	13.51	1.6	1.4	9.8960	2.2	1.9	-	-	5.1962	0.9045
	F2	13.51	1.6	2.8	19.7920	2.2	0.7	8.4823	100	5.1962	2.8090
	T2	13.51	1.6	1.4	9.8960	2.2	1.8	-	-	5.1962	0.9045
S30/K70_01	F1	11.7	1	2.4	16.9646	2.1	1.1	7.0686	140	4.5	2.7699
	T1	11.7	1	0.9	6.3617	2.1	2.5	-	-	4.5	0.4137
S30/K70_02	F1	10.97	2.1	2.2	15.5509	1.3	1.2	0.7069	4.7619	4.2192	2.6857
	T1	10.97	2.1	1.6	11.3097	1.3	1.7	-	-	4.2192	1.6805
	F2	10.97	2.1	2.1	14.8440	1.3	1.35	2.4740	31.25	4.2192	2.5182
	T2	10.97	2.1	1.4	9.8960	1.3	1.9	-	-	4.2192	1.3455
S30/K70_03	F1	11.57	1.6	2.2	15.5509	2.1	1.35	5.3014	37.5	4.45	2.4946
	T1	11.57	1.6	1.25	8.8357	2.1	1.7	-	-	4.45	0.9856
	F2	11.57	1.6	2.3	16.2577	2.1	0.6	7.7754	84	4.45	2.6534
	T2	11.57	1.6	1.2	8.4823	2.1	1.4	-	-	4.45	0.9061

12.4. Appendix D: Heave Ratio and Water Absorption Results

The first two graphs in this appendix show the heave ratio change with respect to the fine content. Figure 12.2 illustrates the heave after the first freezing while Figure 12.3 the after the second freezing.
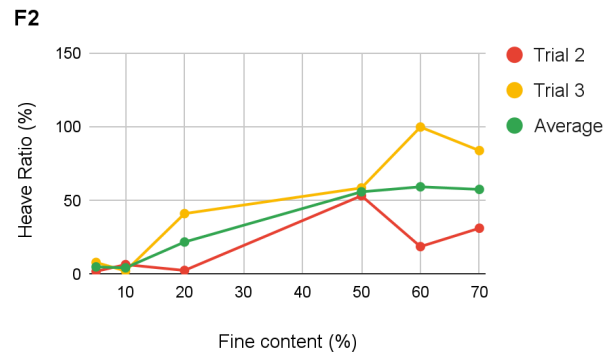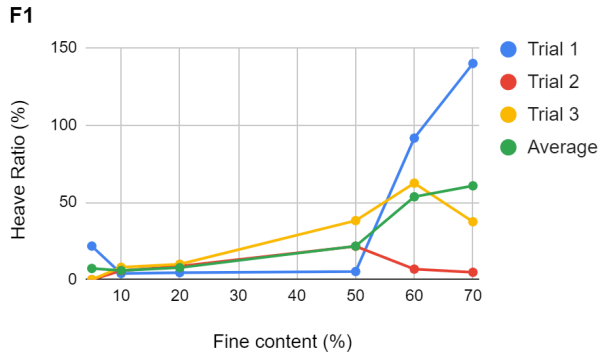

Figure 12.2: Heave ratio vs fines for first freezing   *Figure 12.3: Heave ratio vs fines for second freezing*

During thawing in some of the samples, water leaked through the bottom of the cylindrical containers. From the six figures below it is evident (by the decrease in water height after T1) in which trials and for which samples this had the most effect. These samples were: S80/K20_02, S50/K50_01, S50/K50_02, S40/K60_02 and S30/K70_03. As a consequence of this water loss, the heave ratio, particularly during the second freezing, was heavily impacted. The F2 heave ratio would likely have been higher had the samples been better sealed. It was decided to add water to the samples in which a significant portion of the water film had been lost. The amount added was chosen based on how much water was needed to restore the 1 cm water film after the initial thawing.
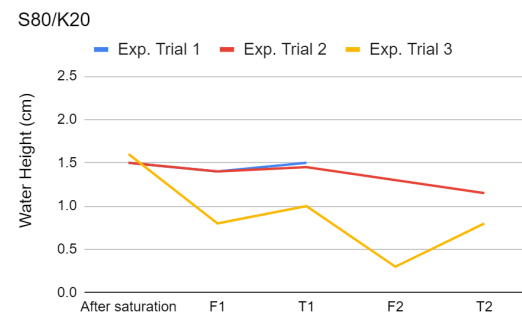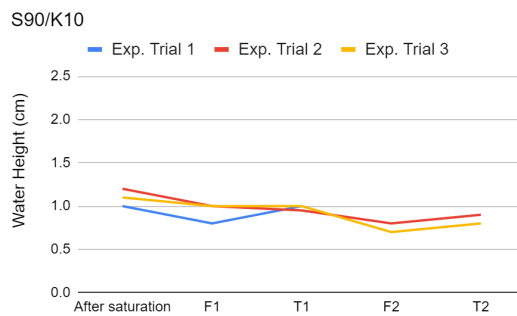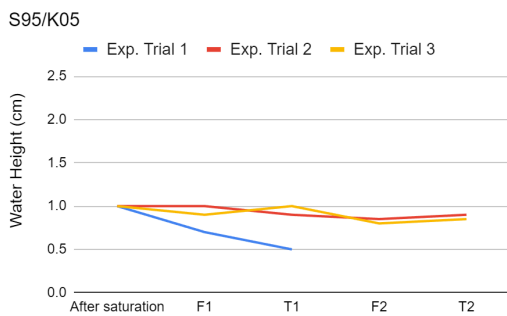
Figures 12.4, 12.5 & 12.6: Water height changes for S95/K05, S90/K10 and S80/K20 samples
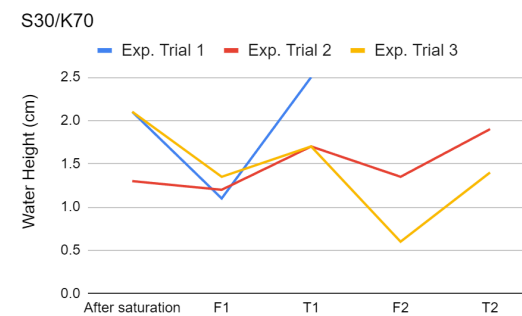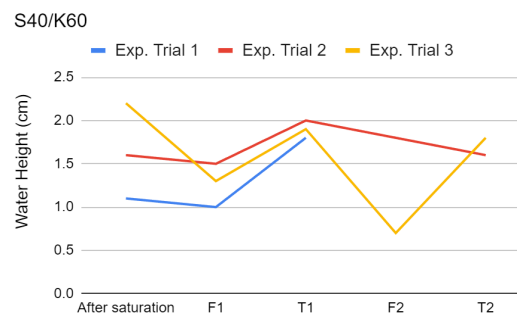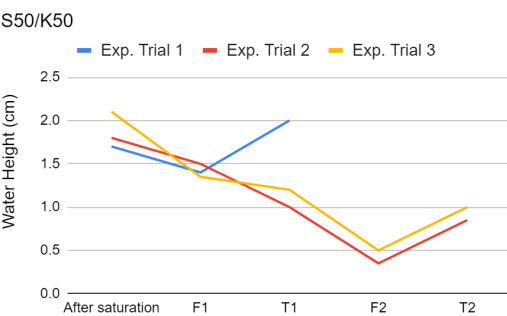
Figures 12.7, 12.8 & 12.9: Water height changes for S50/K50, S40/K60 and S30/K70 samples

In the histogram below a comparison between the 3 trails is provided. On average, the water absorption values are predominantly low, indicating that the decrease in water film height was minimal most of the time. However, when that was not the case, the results were most likely heavily impacted.
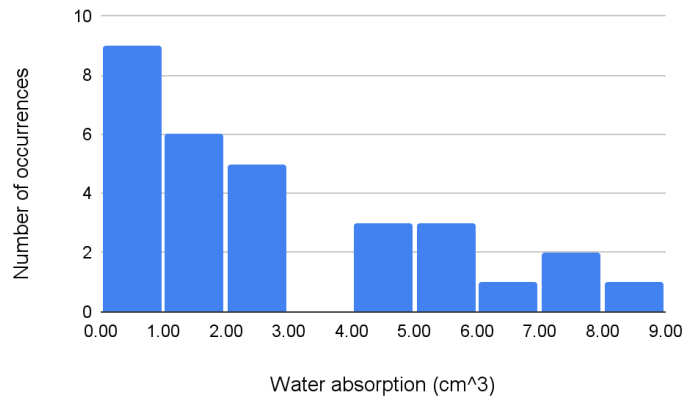
Figure 12.10: Average water absorption for both freezing processes

12.5. Appendix E: Pictures of Samples
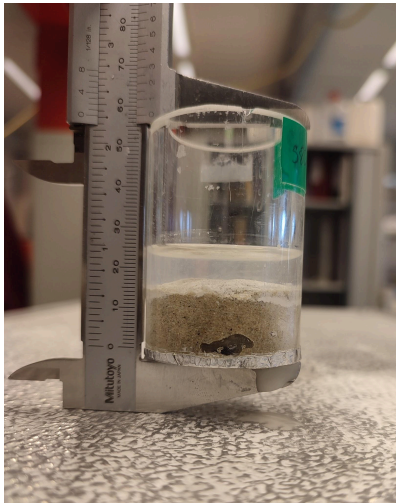
Figure 12.11: S80/K20_03 after 1st thawing process

By looking at the samples from the 2nd and 3rd batches, in the first two sets of figures below, it is visible that after the saturation of the 3rd batch the samples collapsed more and the sand and kaolin in them segregated and formed two different layers. The segregation of the sand and kaolin could have occurred because of a poor mixing process and the different cohesiveness between them.
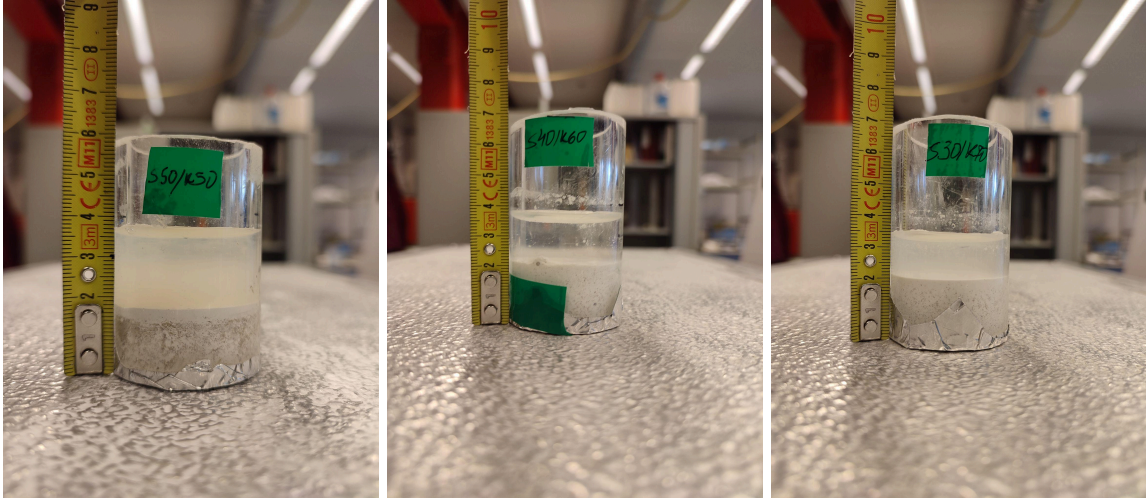
Figures 12.12, 12.13 & 12.14: S50/K50, S40/K60 and S30/K70 samples from second batch after saturation

Figures 12.15, 12.16 & 12.17: S50/K50, S40/K60 and S30/K70 samples from third batch after saturation

The two images below serve as an example to show the lack of ice lenses in the samples with high sand content. This observation holds true for all trials and freezing processes for these two mixtures.
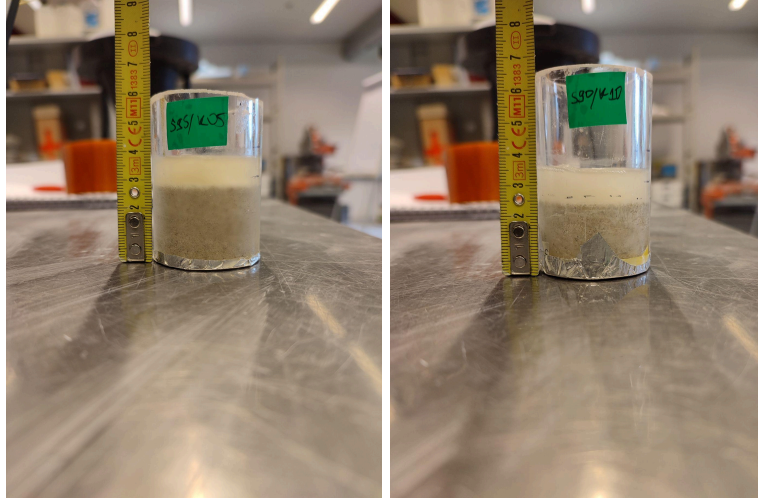
Figures 12.18 & 12.19: S95/K05_01 and S90/K10_01 samples after F1

12.6. Appendix F: Comparative Analysis

The Fiji software is used to estimate the sample heights. Each scan captures a series of images (slices) depicting the samples at various positions within the sample. A total of 11 scans per mixture are available, with the initial scan conducted after the samples were saturated, followed by scans taken after each freeze-thaw cycle. In addition, 6 intermediate scans were performed during the freezing and thawing processes. The scans vary in resolution, corresponding to their respective capture durations: the scans taken after each process have higher resolution due to slower capture, whereas the intermediate scans were faster and hence have lower resolution. The height of the samples in every scan was determined by taking the average value of the maximum and minimum sample height from all the images within one scan as illustrated in Figure 12.20 and Figure 12.21. The height is estimated with the length of the yellow line in the figures which is calculated with the size of the pixels. In the slow scans there are 37 microns/px and in the fast scans 74 microns/px.
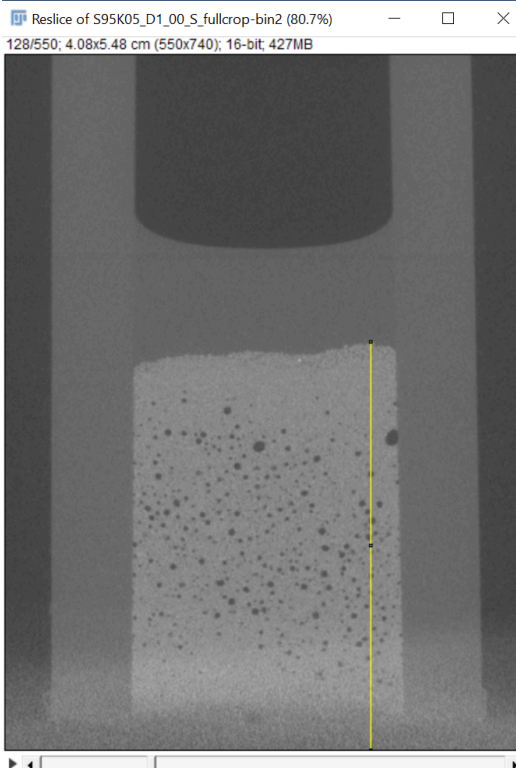
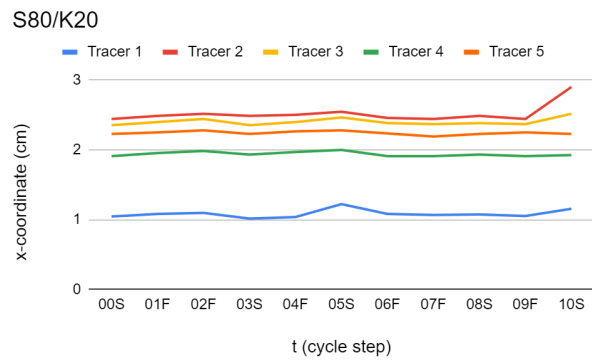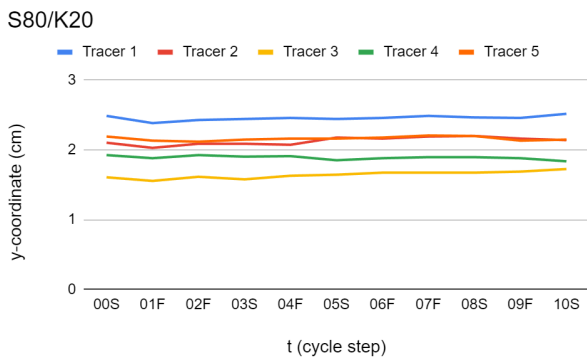*Figure 12.20: Slice with max height for Scan 00S Sample S95/K05*
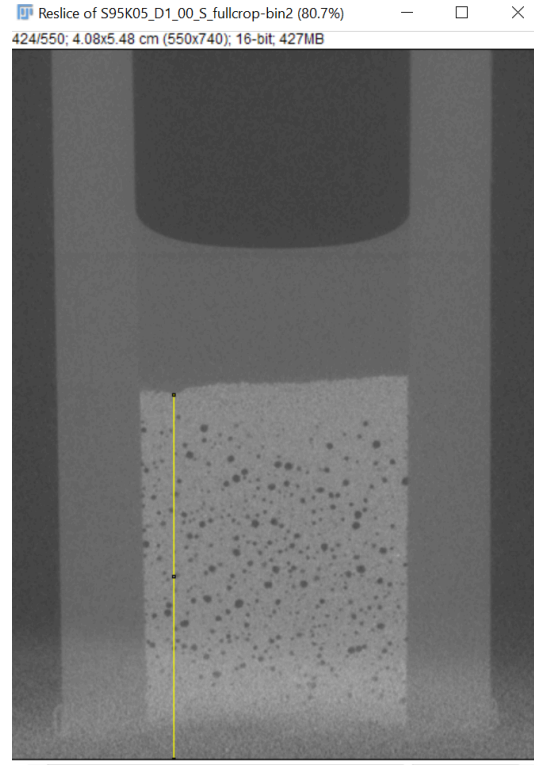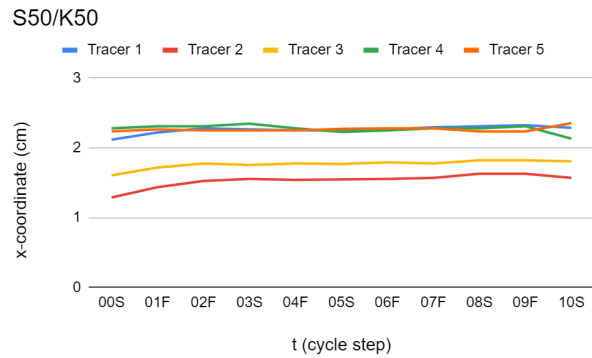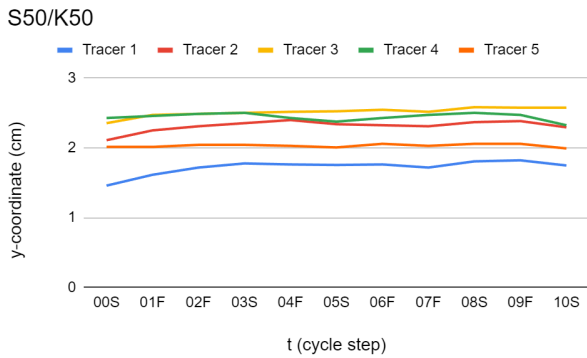

Figure 12.21: Slice with min height for Scan 00S Sample S95/K05
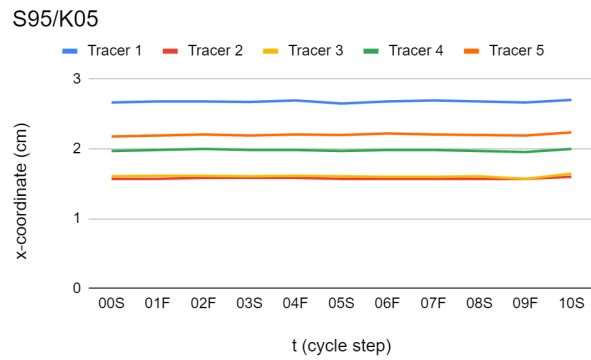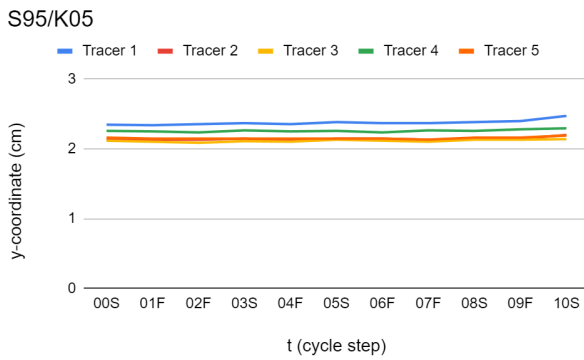
Figures 12.22 & 12.23: Horizontal displacement of the tracers in sample S95/K05
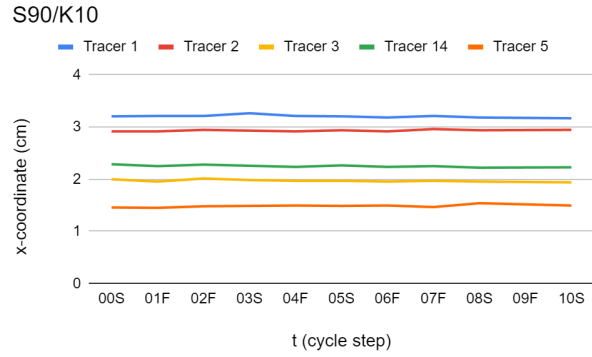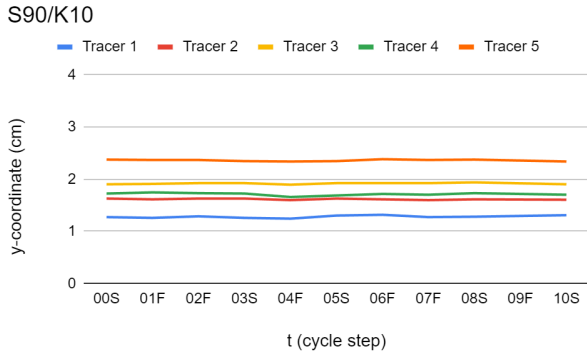
S90/K10

S90/K10

Figures 12.24 & 12.25: Horizontal displacement of the tracers in sample S90/K10

S80/K20

S80/K20

Figures 12.26 & 12.27: Horizontal displacement of the tracers in sample S80/K20

S50/K50

S50/K50

Figures 12.28 & 12.29: Horizontal displacement of the tracers in sample S50/K50

The 3D plots made with python defend what was already established in <u>Chapter 7.2</u>. In all instances, the vertical displacement of the tracers is of a higher magnitude than the horizontal displacement.
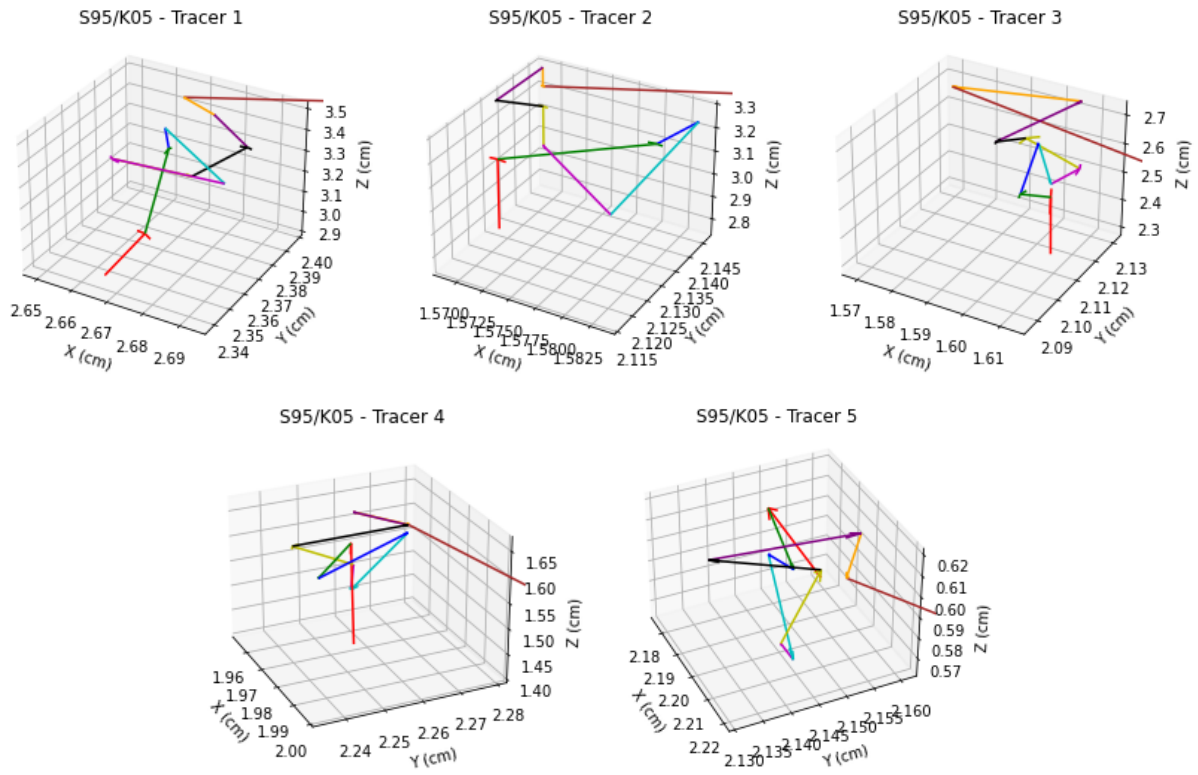

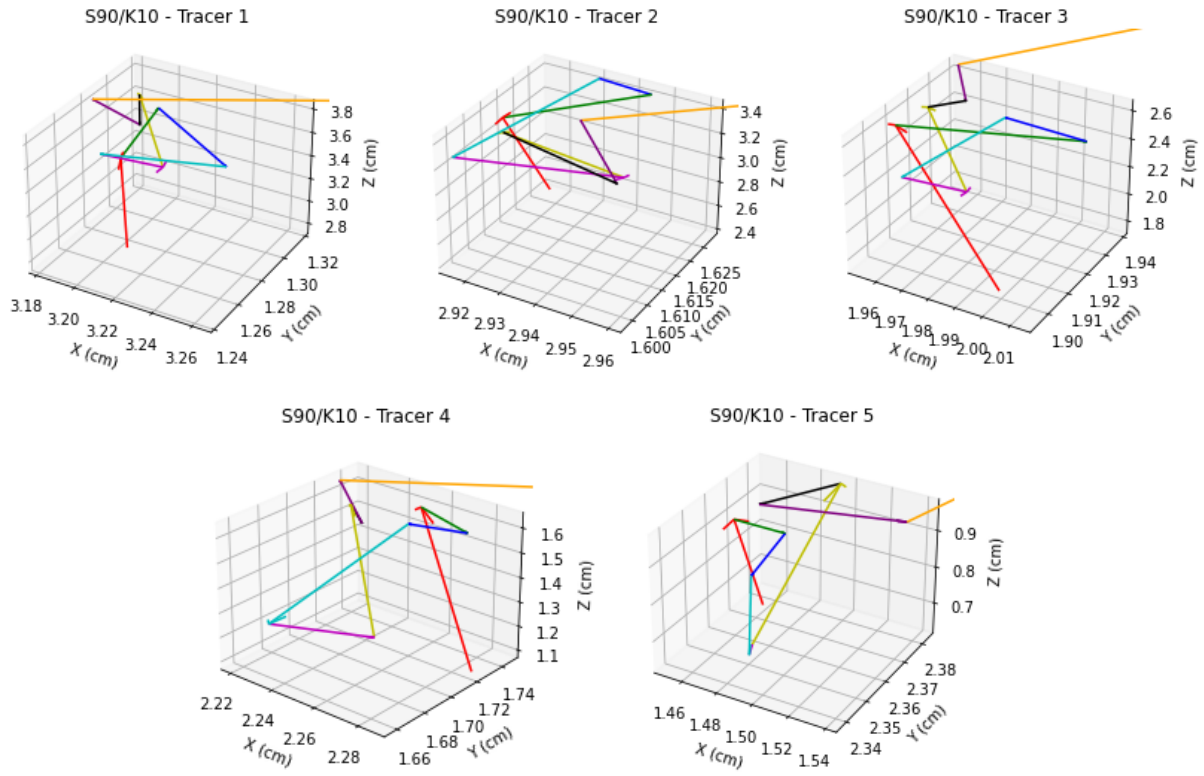*Figure 12.30: 3D displacement of tracers in S95/K05*

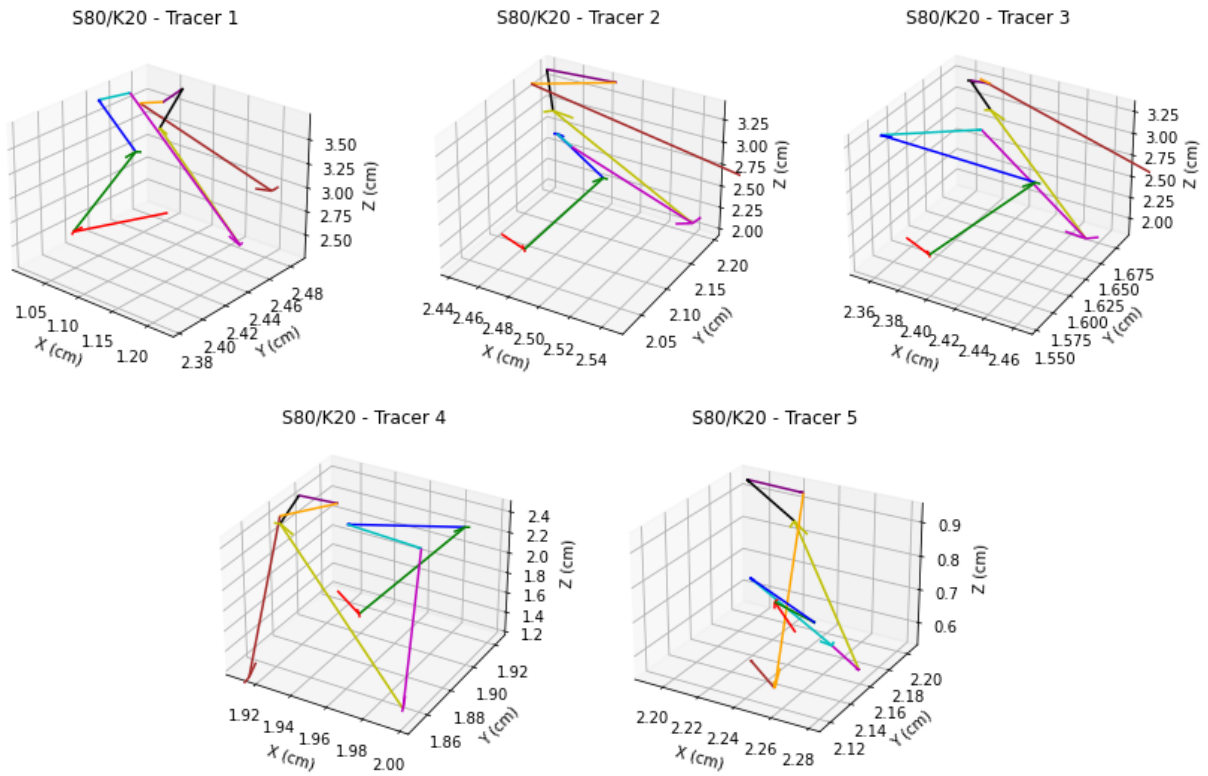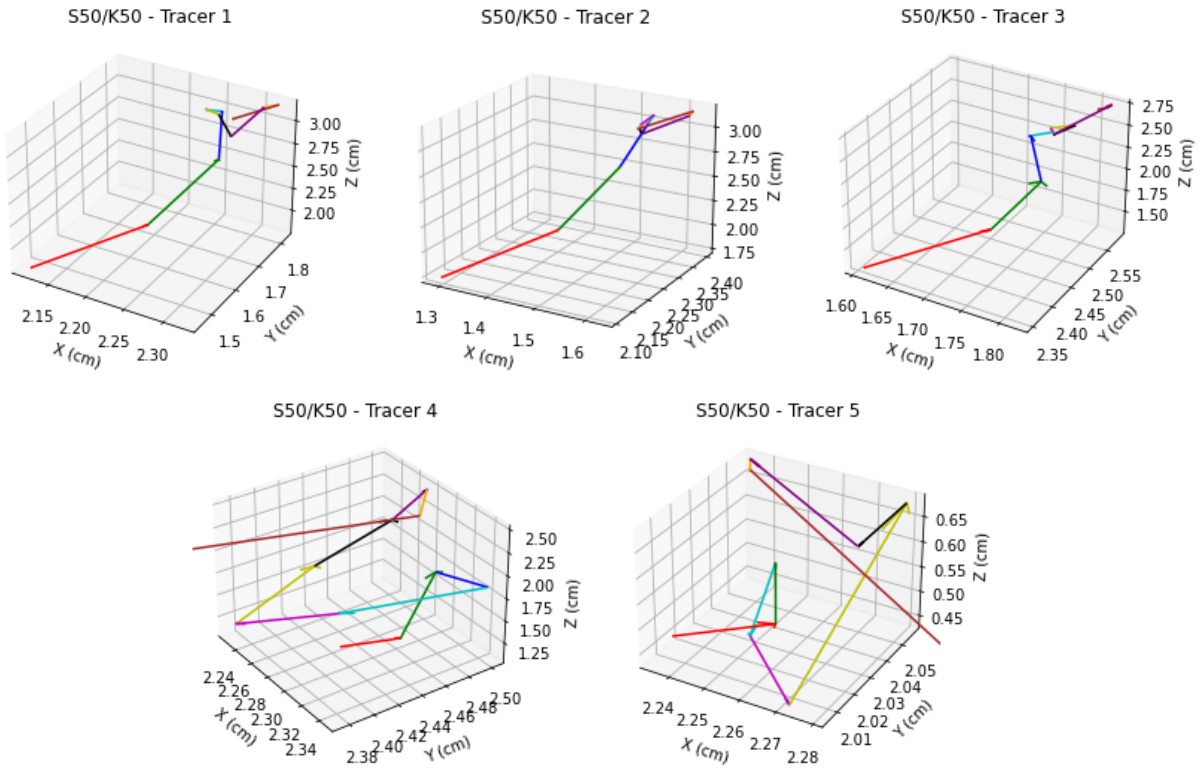*Figure 12.31: 3D displacement of tracers in S90/K10*

Figure 12.32: 3D displacement of tracers in S80/K20

Figure 12.33: 3D displacement of tracers in S50/K50